National Library
of Canada

Acquisitions and
Bibliographic Services Branch

395 Wellington Street
Ottawa, Ontario
K1A 0N4

Bibliothèque nationale
du Canada

Direction des acquisitions et
des services bibliographiques

395, rue Wellington
Ottawa (Ontario)
K1A 0N4

Your file Votre référence

Our file Notre référence

NOTICE

The quality of this microform is heavily dependent upon the quality of the original thesis submitted for microfilming. Every effort has been made to ensure the highest quality of reproduction possible.

If pages are missing, contact the university which granted the degree.

Some pages may have indistinct print especially if the original pages were typed with a poor typewriter ribbon or if the university sent us an inferior photocopy.

Reproduction in full or in part of this microform is governed by the Canadian Copyright Act, R.S.C. 1970, c. C-30, and subsequent amendments.

AVIS

La qualité de cette microforme dépend grandement de la qualité de la thèse soumise au microfilmage. Nous avons tout fait pour assurer une qualité supérieure de reproduction.

S'il manque des pages, veuillez communiquer avec l'université qui a conféré le grade.

La qualité d'impression de certaines pages peut laisser à désirer, surtout si les pages originales ont été dactylographiées à l'aide d'un ruban usé ou si l'université nous a fait parvenir une photocopie de qualité inférieure.

La reproduction, même partielle, de cette microforme est soumise à la Loi canadienne sur le droit d'auteur, SRC 1970, c. C-30, et ses amendements subséquents.

Canada

UNIVERSITY OF ALBERTA

HOLLOW MICROSTRUCTURAL WAVEGUIDES OF CIRCULAR CROSS-SECTION FOR PROPAGATION OF INFRARED RADIATION

by

TING WANG

(C)

A THESIS

SUBMITTED TO THE FACULTY OF GRADUATE STUDIES AND RESEARCH

IN PARTIAL FULFILLMENT OF THE REQUIREMENTS FOR THE DEGREE OF

MASTER OF SCIENCE

DEPARTMENT OF ELECTRICAL ENGINEERING

EDMONTON, ALBERTA

FALL 1992

National Library of Canada
Bibliothèque nationale du Canada

Canadian Theses Service
Service des thèses canadiennes

Ottawa, Canada
K1A 0N4

The author has granted an irrevocable non-exclusive licence allowing the National Library of Canada to reproduce, loan, distribute or sell copies of his/her thesis by any means and in any form or format, making this thesis available to interested persons.

L'auteur a accordé une licence irrévocable et non exclusive permettant à la Bibliothèque nationale du Canada de reproduire, prêter, distribuer ou vendre des copies de sa thèse de quelque manière et sous quelque forme que ce soit pour mettre des exemplaires de cette thèse à la disposition des personnes intéressées.

The author retains ownership of the copyright in his/her thesis. Neither the thesis nor substantial extracts from it may be printed or otherwise reproduced without his/her permission.

L'auteur conserve la propriété du droit d'auteur qui protège sa thèse. Ni la thèse ni des extraits substantiels de celle-ci ne doivent être imprimés ou autrement reproduits sans son autorisation.

ISBN 0-315-77318-9

Canada

UNIVERSITY OF ALBERTA

RELEASE FORM

NAME OF AUTHOR: TING WANG

TITLE OF THESIS: HOLLOW MICROSTRUCTURAL WAVEGUIDES OF CIRCULAR CROSS-SECTION FOR PROPAGATION OF INFRARED RADIATION

DEGREE: MASTER OF SCIENCE

YEAR THIS DEGREE GRANTED: 1992

Permission is hereby granted to the University of Alberta Library to reproduce single copies of this thesis and to lend or sell such copies for private, scholarly or scientific research purpose only.

The author reserves all other publication and other right in association with the copyright in the thesis, and except as hereinbefore provided neither the thesis nor any substantial portion thereof may be printed or otherwise reproduced in any material form whatever without the author's prior written permission.

Ting Wang

Date: May 5, 1992

Ting Wang
c/o Liu ZhenZheng
Second Inpatient Dept.
Second Hospital
Harbin Medical University
Harbin, Heilongjiang, China

UNIVERSITY OF ALBERTA

FACULTY OF GRADUATE STUDIES AND RESEARCH

THE UNDESIGNED CERTIFY THEY HAVE READ, AND RECOMMEND TO THE FACULTY OF GRADUATE STUDIES AND RESEARCH FOR ACCEPTANCE, A THESIS ENTITLED **HOLLOW MICROSTRUCTURAL WAVEGUIDES OF CIRCULAR CROSS-SECTION FOR PROPAGATION OF INFRARED RADIATION** SUBMITTED BY **TING WANG** IN PARTIAL FULFILLMENT OF THE REQUIREMENTS FOR THE DEGREE OF **MASTER OF SCIENCE**

.....
Dr. C.R. James (Supervisor)

.....
Dr. F.E. Vermeulen (Supervisor)

.....
Dr. A.M. Robinson (Supervisor)

.....
Dr. J.N. McMullin

.....
Dr. W. Rozmus

date: April 27, 1992

DEDICATED

To my wife Shaohua

ABSTRACT

Theoretical estimates are given of the propagation losses of infrared radiation in micron-sized hollow cylindrical waveguides by analyzing the characteristic (determinantal) equation of two-medium wave guiding systems of circular cross-section. The gold-coated wall of the guide is the exterior medium and the hollow region within the guide is the interior medium.

Propagation characteristics of the three types of modes existing in such waveguides are described. These modes are the TE, TM and hybrid modes. The TE_{01} mode is shown to have the most loss-free propagation due to the small tangential components of electric fields at the gold-coated surface.

Numerical solutions of the determinantal equation have been obtained, which confirm the theoretical predictions.

Both theoretical and numerical results suggest that wave transmission is possible over a significant number of wavelengths.

For the most loss-free cases, the losses are expected to be of the order of 0.1dB/cm.

ACKNOWLEDGEMENT

The author would like to express his sincere thanks to his supervisors, Dr. C.R. James, Dr. F.E. Vermeulen and Dr. A.M. Robinson for their invaluable help, continuous encouragement and direction during the course of this project. He also wishes to extend special appreciation to Dr. R.P.W.Lawson for his concerns, efforts and support throughout the work.

The author is very grateful to Dr. J. McMullin for discussions which have been extremely stimulating and immensely contributive.

The help of Dr. C. Stroemich in introducing the author to the Macintosh computer system is greatly appreciated.

Finally, the author would like to express his indebtedness to his wife. Well-deserved gratitude goes to her for her understanding and patience.

TABLE OF CONTENTS

Chapter	Page
1. INTRODUCTION	1
2. REVIEW	4
3. MATHEMATICAL PREPARATION	7
3.1 Complex Refractive Index	7
3.2 Determinantal Equation	11
3.3 Analysis of Perfect Conductor Waveguides	22
4. ANALYTICAL RESULTS FOR CYLINDRICAL MICROSTRUCTURAL WAVEGUIDES	25
4.1 General Comments	25
4.2 Designation of Modes	29
4.3 Simplification of Determinantal Equation	34
4.4 Characteristics of TE Modes	38
4.5 Characteristics of TM Modes	46
4.6 Characteristics of Hybrid Modes	48
5. NUMERICAL RESULTS FOR CYLINDRICAL MICROSTRUCTURAL WAVEGUIDES	54
5.1 Numerical Methodology	54
5.2 Asymptotic Behavior of Hankel Functions	59

5.3 Numerical Results for TE_{01} Mode 61

5.4 Numerical Results for TM_{01} Mode 64

5.5 Numerical Results for a Hybrid Mode 68

6. CONCLUSIONS 72

REFERENCES 92

APPENDIX 96

LIST OF FIGURES

Figure Page

Fig.1 Geometry of Cylindrical Microstructural Waveguide 77

Fig.2 Bessel Functions $J_0(K_d r)$ and $J_1(K_d r)$ 78

Fig.3 Hankel Functions $H_0^{(2)}(K_m r)$ and $H_1^{(2)}(K_m r)$ 78

Fig.4 Illustration of Muller's Method 79

Fig.5 Propagation Distance of the TE_{01} Mode at 1.033μm 80

Fig.6 Propagation Distance of the TE_{01} Mode at 9.919μm 80

Fig.7 Attenuation Constant of the TM_{01} Mode at 1.033μm 81

Fig.8 Propagation Distance of the TM_{01} Mode at 1.033μm 81

Fig.9 Attenuation Constant of the TM_{01} Mode at 9.919μm 82

Fig.10 Propagation Distance of the TM_{01} Mode at 9.919μm 82

Fig.11 Radial Variation of E_{zd} of the Ideal Lossless Waveguide for the TM_{01} Mode 83

Fig.12 Radial Variation of E_{zd} of the Microstructural Waveguide for the TM_{01} Mode at 1.033μm and $a/\lambda_o=1$ 84

Fig.13 Radial Variation of E_{zd} of the Microstructural Waveguide for the TM_{01} Mode at 1.033μm and $a/\lambda_o=20$ 84

Fig.14 Radial Variation of E_{zd} of the Microstructural Waveguide for the TM_{01} Mode at 9.919μm and $a/\lambda_o=1$ 85

Fig.15 Radial Variation of E_{zd} of the Microstructural Waveguide for the TM_{01} Mode at 9.919μm and $a/\lambda_o=20$ 85

Fig.16 Attenuation Constant of the Hybrid Mode at 1.033μm 86

Fig.17 Propagation Distance of the Hybrid Mode at 1.033μm 86

Fig.18 Attenuation Constant of the Hybrid Mode at 9.919μm 87

Fig.19 Propagation Distance of the Hybrid Mode at 9.919μm 87

Fig.20 Radial Variation of $E\phi_d$ of the Ideal Lossless Waveguide for the TE_{11} Mode 88

Fig.21 The Magnitude of $J_1'(K_d r)$ of the Microstructural Waveguide for the Hybrid Mode at 1.033μm and $a/\lambda_o=2$ 89

Fig.22 The Magnitude of $J_1'(K_d r)$ of the Microstructural Waveguide for the Hybrid Mode at 1.033μm and $a/\lambda_o=3$ 89

Fig.23 The Magnitude of $J_1'(K_d r)$ of the Microstructural Waveguide for the Hybrid Mode at 9.919μm and $a/\lambda_o=18$ 90

Fig.24 The Magnitude of $J_1'(K_d r)$ of the Microstructural Waveguide for the Hybrid Mode at 9.919μm and $a/\lambda_o=19$ 90

Fig.25 Magnitude of R for the Hybrid Mode at 1.033μm 91

Fig.26 Magnitude of R for the Hybrid Mode at 9.919μm 91

LIST OF TABLES

TABLES	Page
TABLE I	75
TABLE II	76
TABLE III	76

1 INTRODUCTION

In recent years, silicon micromachining technology has become capable of producing a variety of mechanical microstructures for sensor and actuator applications[1]-[6]. These microstructures actually enable relatively accurate measurements of force, vibration, acceleration, resistance, displacement, and vapor concentration. Another application of these structures is in the production of dielectric-filled channel optical waveguides, as proposed by Miller[7] in 1969, as basic components in integrated optics.

Since then much research [8]-[14] has been done in the area of channel optical waveguides utilizing micromachining. There are two basic channel waveguide structures, the ridge structure and the imbedded structure. Those devices are micrometer-sized, but are dielectric waveguides with no hollow regions. Recently a new technique of fabricating vacuum microelectronic devices by microstructural technology has been introduced[15], [16].

In this thesis we consider hollow waveguides with gold-coated surfaces. Few investigations have been done on the field propagation in microstructural hollow metal waveguides, probably due to the expected large losses originating from the large circumference of such waveguides in relation to the cross sectional area. In this thesis, the hollow cylindrical waveguides will be shown to be attractive

as an optical transmission medium. We will show that the propagation distances of infrared radiation in these hollow microstructures are significant in relation to distances measured on a die, although not in relation to distances that are of interest in optical fiber transmission.

The hollow metallic microstructural waveguides are expected to have potential applications in such areas as sensors, opto-electronic components and optical computers. An important aspect of hollow optical guides is the empty region. This region is indispensable for the wave-beam interaction devices which may now be possible using the newly fabricated vacuum microelectronic devices. Such miniature vacuum tubes are vacuum-switching and power-control devices which are completely analogous to existing microwave vacuum tubes. What makes them different is that they are micrometer-sized devices and they are fabricated on a silicon wafer using integrated-circuit fabrication techniques.

The existing techniques make it possible to fabricate such micro-guides with triangular, rectangular or trapezoidal cross-sections. We can control the waveguide profile and reproduce it with great accuracy. The dimensional precision and structural smoothness can be satisfactorily obtained by etching along crystal planes. Even though it is not practical at this time to fabricate a microstructural waveguide with circular cross-section, the

analysis of circular guides is still very important. Only parallel-plate guides of infinite extent, i.e. " open system" waveguides, have been investigated to date[22]. There is no published investigation about the "closed system" waveguides in which the cross-sectional areas are completely enclosed by the waveguide walls. The analysis of microstructural waveguides of triangular, rectangular or trapezoidal cross sections will be extremely difficult. But it is expected that cylindrical waveguides will be theoretically less difficult to analyze and these waveguides can still yield very important information about the propagation characteristics of "closed system" waveguides.

The objective of this thesis is to present an analysis of the propagation characteristics of some cylindrically symmetric TM and TE modes and a hybrid mode in hollow gold-coated cylindrical microstructural waveguides for infrared wavelengths of 1-10μm. Gold is chosen as a coating material because it has high reflectance for infrared radiation. The analysis is carried out by approximate analytical methods and precise numerical methods. It will be shown that infrared radiation can propagate along such waveguides for a significant number of wavelengths for some modes, but not for others. In general the losses are larger than those of ridge and imbedded dielectric waveguides.

2 REVIEW

Nearly 60 years ago Carson *et al.*[17] proposed circular cross-section waveguides for microwave (wavelength range of 1 millimeter to 1 meter) transmission. They proved that for such a waveguide where the bounding surface is perfectly conducting, there are two types of modes of waves. For waves that contain only an electric field but no magnetic field in the direction of propagation, the magnetic field lies entirely in the transverse plane; they are known as transverse magnetic(TM) waves. They have also been referred to in the literature as E-waves, or waves of the electric type. On the other hand, waves that contain a magnetic field but no electric field in the direction of propagation are known as transverse electric(TE) waves, and have been also referred to as H-waves or waves of the magnetic type.

For microwave cylindrical waveguides, only TM or TE modes of waves exist, due to the boundary condition that the tangential components of the electric field at the guide-walls are close to zero. A material is called a good conductor if such a boundary condition is valid. At microwave frequencies, metals can be viewed as perfect conductors in any practical sense.

Attenuation constants were derived in [17] by calculating the ratio of the average power transmitted by the guide and the average power loss in the walls per unit

length of guide. From this ratio, the attenuation can be readily obtained.

Another method was pointed out in [17]; a waveguide can be considered as a two medium system, with the air inside the guide as one medium, and the guide walls as the other. The electric fields and the magnetic fields in both media can be obtained. By matching these fields on the boundary, an equation can be derived. The equation, referred to as the determinantal equation or the characteristic equation, contains the information necessary to calculate wave propagation and characteristics.

The work of these authors, however, was restricted to propagation of radio-frequency waves.

The work on optical waveguides received much impetus from the advent of lasers in the early 1960s. Marcatilli and Schmeltzer[18], were the first to investigate large optical waveguides of circular cross-section in 1964. The field configurations and propagation constants of the normal modes were determined for a hollow circular waveguide made of dielectric or metal. For a wavelength λ_o=1μm and a radius a=0.25mm, the attenuation for the minimum loss TE_{01} modes in an aluminum waveguide was calculated to be only 1.8 db/km.

About 10 years later, other researchers[19]-[21], obtained propagation characteristics of large optical waveguides of parallel plates and rectangular cross-sections. In such waveguides, the dimensions of the

waveguides are much larger than the free space wavelengths.

The only investigation on the hollow microstructural waveguides fabricated on silicon by micromachining techniques was published by Vermeulen, *et al.*[22]. They investigated micron-sized parallel plate waveguides. In [22], theoretical results are presented on the propagation of infrared radiation in micronsized parallel plane waveguides whose walls are gold-coated and separated by empty space. Propagation characteristics of the TM_{10}, TE_{10}, and TEM modes are described. The results, when extrapolated to propagation in hollow micron-sized waveguides of rectangular cross section, suggest that propagation is possible over a significant number of wavelengths in spite of the large circumference of such guides in relation to their cross sectional area. Theoretical indications are that the most loss-free structures have losses of the order of 0.1db/cm.

In this thesis, we will use an approach similar to that used in [22], adapted for cylindrical waveguides.

3 MATHEMATICAL PREPARATION

3.1 Complex Refractive Index

Maxwell's equations are a comprehensive summary of the laws of electromagnetism. They convey to us all the classical information about electromagnetic phenomena and should, in principle, be taken as a starting point for solutions of any problems in classical electromagnetic theory. In practice, however, this is often not done for various reasons. The geometry of the material bodies present may not be easily expressed in any co-ordinate system, making the complete solution extremely difficult; or one may only be interested in investigating a single mode, e.g. the transmission-line mode which can be treated by network theory. However, whenever it is possible it is desirable to use the approach from Maxwell's equations since in this way a complete set of solutions can be obtained. Even though only one mode may be used in practice, it is often helpful to know how the other modes behave, if only for the purpose of avoiding them.

Maxwell's equations in MKS units are , in their most general form,

$$\nabla \cdot \mathbf{D} = \rho$$

$$\nabla \cdot \mathbf{B} = 0$$

$$\nabla \times \mathbf{H} = \sigma \mathbf{E} + \frac{\partial \mathbf{D}}{\partial t}$$

$$\nabla \times \mathbf{E} = - \frac{\partial \mathbf{B}}{\partial t}$$

Here ρ is the charge density and σ is the conductivity of the medium at the point. Here and in all work that follows, the MKS system of units is employed. We have further relations, for all media,

$$\mathbf{D} = \varepsilon \mathbf{E}$$

$$\mathbf{B} = \mu \mathbf{H}$$

where ε and μ are the permittivity and permeability of the material, respectively. In general μ is a real constant for non-magnetic materials as is the case in this thesis, and ε may be a complex scalar. They are denoted as ε_o and μ_o in vacuum.

If the time variation can be represented in the form $e^{j\omega t}$, where ω = radian frequency and t = time, then $\partial/\partial t \equiv j\omega$,

and, $$\nabla \times \mathbf{H} = j\omega(\varepsilon - j\frac{\sigma}{\omega})\mathbf{E} \ .$$

The term in the bracket of the right hand side can be considered as a complex dielectric constant, which we denote as ε_c, and thus

$$\varepsilon_c = \varepsilon - j\frac{\sigma}{\omega} \ .$$

It is customary to express ε_c as

$$\varepsilon_c = \varepsilon' - j\varepsilon''$$

where $\varepsilon' = \varepsilon$, $\varepsilon'' = \frac{\sigma}{\omega}$.

Assuming the axis of the cylindrical waveguide is in the z direction, we have

$$E_z = f(r,\phi)e^{j\omega t}e^{-\gamma z}$$

where $f(r,\phi)$ is a function of radius r and azimuthal angle ϕ only, and γ is called the propagation constant. It is a complex number, so $\gamma = \alpha + j\beta$. The electric field becomes smaller with z by the factor $e^{-\alpha z}$, where α is called the attenuation constant, β the phase constant, which is a measure of the phase shift with z.

If we use light-wave terminology, the complex refractive index of a medium can be expressed as

$$N=n-jk$$

where n= index of refraction, k = extinction coefficient.

The electric field intensity, E, of a plane wave propagating in the direction of the z-axis in this medium can be described in terms of the complex refractive index $N=n-jk$ as[24],

$$E=Eoe^{j(\omega t+\phi)}\ e^{-j(\omega/c)Nz}$$

$$=Eoe^{j(\omega t+\phi)}\ e^{-j(\omega/c)nz}\ e^{-(\omega/c)kz}$$

$$=Eoe^{j(\omega t+\phi)}\ e^{-j\beta z}\ e^{-\alpha z} \quad .....(3.1.1)$$

where Eo= wave amplitude

ϕ= phase angle

c= velocity of light in free space.

Using the terminology of microwave engineering, the same wave may be expressed as,

$$E=E_o e^{j(\omega t+\phi)} e^{-\gamma z}. \qquad .....(3.1.2)$$

Thus, from (3.1.1) and (3.1.2), we have,

$$-j\frac{\omega}{c} N z = -\gamma z = -j\omega\sqrt{\mu\varepsilon_c}\, z .$$

By knowing $\sqrt{\mu\varepsilon_c} = \sqrt{\mu\varepsilon_o}\ \sqrt{\varepsilon_c/\varepsilon_o}$, and $c=1/\sqrt{\mu\varepsilon_o}$ which is the speed of light in free space, for non-magnetic material, where $\mu=\mu_o$, we obtain,

$$N=n-jk=\sqrt{\varepsilon_c/\varepsilon_o}$$

where ε_o is the permittivity of free space.

From the above it may be shown that

$$\frac{\varepsilon'}{\varepsilon_o} = n^2-k^2$$

$$\frac{\varepsilon''}{\varepsilon_o} = 2nk .$$

In order to discuss the attenuation characteristics of metallic microstructural waveguides, we will need to have some quantitative information about the behavior of metals at optical frequencies.

Because we are investigating propagation of infrared radiation in microstructural waveguides, we are only interested in wavelengths from 1μm to 10μm.

Values of the complex refractive index of gold can be converted to complex permittivity for a range of free space wavelengths λ_o between 1μm and 10μm from published values of n and k for evaporated gold films[25]. Some values are tabulated in TABLE I.

From the TABLE I we can see that, for the wavelengths of interest in this thesis,

$$\left|\frac{\varepsilon_c}{\varepsilon_o}\right| = |N^2| = |(n-jk)^2| \gg 1 \ .$$

This is the fact which we will use frequently in the later part of this thesis.

Since

$$|E| = e^{-(\omega/c)kd}$$

it can be shown that a plane wave propagating in gold will decay to 1/e of its initial value in a distance of approximately d=0.025μm. Therefore a gold film of thickness equal to a small fraction of a micron is adequate for coating the walls of a microstructural waveguide.

3.2 Determinantal Equation

We derive here the determinantal equation; the procedure that is followed is outlined in the paragraphs that follow.

Maxwell's equations are taken as a starting point. From these, a pair of wave equations are derived, containing E_z and H_z, where z is the direction of wave propagation. Solution of the wave equations gives E_z and H_z in terms of certain arbitrary constants and the propagation constant γ. The other field components are obtained from Maxwell's equations in terms of E_z and H_z. By applying boundary conditions, a number of equations containing the arbitrary constants are obtained. If the same number of boundary conditions are taken as there are constants, these constants can be eliminated to give an equation involving the propagation constant γ as the only unknown.

In the analysis of the propagation characteristics in the micron-sized waveguides, the gold and free space regions are initially treated as two general dielectric media with complex permeability μ_m and μ_d, and complex permittivity ε_m and ε_d, respectively. The geometry of the waveguide is shown in Fig.1.

We will describe the waves propagating along the waveguide in terms of a propagation factor $e^{j\omega t-\gamma z}$.

The wave equations in the two media can be written as[23]

$$\nabla^2 \mathbf{E}+k^2\mathbf{E}=0$$

$$\nabla^2 \mathbf{H}+k^2\mathbf{H}=0$$

where $k^2=\omega^2\mu\varepsilon_c$, which depends upon the medium.

The z-components of those equations in a cylindrical coordinate system are:

$$\frac{1}{r}\frac{\partial}{\partial r}\left(r\frac{\partial Ez}{\partial r}\right) + \frac{1}{r^2}\frac{\partial^2 Ez}{\partial \phi^2} + \frac{\partial Ez}{\partial z^2} + k^2 Ez = 0$$

$$\frac{1}{r}\frac{\partial}{\partial r}\left(r\frac{\partial Hz}{\partial r}\right) + \frac{1}{r^2}\frac{\partial^2 Hz}{\partial \phi^2} + \frac{\partial Hz}{\partial z^2} + k^2 Hz = 0 \ .$$

Because we are looking for the solutions of this equation with a propagation constant described by the factor $e^{-\gamma z}$, we obtain:

$$r\frac{\partial}{\partial r}\left(r\frac{\partial Ez}{\partial r}\right) + \frac{\partial^2 Ez}{\partial \phi^2} + r^2(\gamma^2+k^2)Ez = 0$$

$$r\frac{\partial}{\partial r}\left(r\frac{\partial Hz}{\partial r}\right) + \frac{\partial^2 Hz}{\partial \phi^2} + r^2(\gamma^2+k^2)Hz = 0 \ .$$

Letting $\gamma^2 + k^2 = K^2$ and solving the equation by the method of separation of variables, we get[23],

$$\left.\begin{matrix} Ez \\ Hz \end{matrix}\right\rangle \longrightarrow = PFe^{-\gamma z}$$

where $$P = SJ_m(Kr)+TY_m(Kr)$$

$$F = V\cos(m\phi) + W\sin(m\phi) \ .$$

Here, S, T, V and W are undetermined constants, J_m is the Bessel function of the first kind, and Y_m is the Bessel

function of the second kind[23]. This is the solution of the most general form for both r≥a and r≤a.

In the free space region (letting $K_d^2=\gamma^2+\omega^2\mu_d\varepsilon_d$ and we would like to remind the readers here that in this region $\mu_d=\mu_o$, $\varepsilon_d=\varepsilon_o$) $Y_m(K_dr)$ is excluded as a solution, because the fields must be finite on the axis of the waveguide , and $Y_m(0)=\infty$. Consequently the wave functions within the hollow region should be constructed from the Bessel function of the first kind. Thus we have,

$$E_{zd}=A_m J_m(K_dr) (C_1\cos(m\phi)+C_2\sin(m\phi))e^{-\gamma z} \quad .....(3.2.1)$$

$$H_{zd}=B_m J_m(K_dr) (C_3\cos(m\phi)+C_4\sin(m\phi))e^{-\gamma z}. \quad .....(3.2.2)$$

In Fig.2, $J_o(K_dr)$ and $J_1(K_dr)$ are plotted for reference.

In the metal region (letting $K_m^2=\gamma^2+\omega^2\mu_m\varepsilon_m$), we should mention here that the function $P = SJ_m(Kr)+TY_m(Kr)$ can represent any cylindrical functions including Hankel functions. P must be chosen to ensure the proper behavior of the solution at infinity. The electromagnetic fields should behave as a wave propagating in the positive r direction in the limit as $r \longrightarrow \infty$.

We choose the Hankel function of the second kind as the solution in the metal because for large values of $|K_mr|$, the Hankel functions can be replaced by their asymptotic

forms. Neglecting constant multiplying factors, we have,

$$H_m^{(1)}(K_m r) \propto \exp(jK_m r)/\sqrt{K_m r}$$

$$H_m^{(2)}(K_m r) \propto \exp(-jK_m r)/\sqrt{K_m r} \ .$$

Because $\exp(-jK_m r)$ represent a wave going out from the axis in the radial direction, $H_m^{(2)}(K_m r)$ gives the proper dependence and so is chosen as the radial dependence function. As mentioned above the wave propagating in the positive z-direction has the factor $\exp(-\gamma z)$ and both real and imaginary parts of γ are positive. Therefore because of the factor $\exp(-\gamma z)$, we select the square root of K_m^2 so that K_m lies in the 4th quadrant. This will ensure the wave decays exponentially with distance r.

Thus in the metal region we have,

$$E_{zm}=C_m H_m^{(2)}(K_m r)(C_5\cos(m\phi) + C_6\sin(m\phi))e^{-\gamma z} \quad .....(3.2.3)$$

$$H_{zm}=D_m H_m^{(2)}(K_m r)(C_7\cos(m\phi) + C_8\sin(m\phi))e^{-\gamma z} .....(3.2.4)$$

We plot $|H_0^{(2)}(K_m r)|$ and $|H_i^{(2)}(K_m r)|$ in Fig.3 for reference.

For a boundary surface between two media of finite conductivity of any kind, the component of field intensity (electric or magnetic) parallel to the surface is continuous

at the surface; i.e. when the surface is approached from either side, the values of the components of the fields at the surface are the same.

The boundary conditions which will be satisfied are:

$$E_{zd}=E_{zm}\,|_{r=a} \qquad H_{zd}=H_{zm}|_{r=a}$$

$$E\phi_d=E\phi_m|_{r=a} \qquad H\phi_d=H\phi_m|_{r=a}$$

As evident from (3.2.6), (3.2.8) below, if $E\phi_d=E\phi_m|_{r=a}$ and $H\phi_d=H\phi_m|_{r=a}$ are to be satisfied, every pairs of the above boundary conditions must have the same ϕ-dependence. Thus if the longitudinal electric field in (3.2.1) and (3.2.3) varies with ϕ as $\cos(m\phi)$, then the longitudinal magnetic field in (3.2.2) and (3.2.4) has $\sin(m\phi)$ for its ϕ-dependence. We could also let E_z have a $\sin(m\phi)$ ϕ-dependence and choose $\cos(m\phi)$ for H_z. Because of the axial symmetry of the waveguide, the solution resulting from the latter ϕ-dependence would differ from the first only by a rotation of the fields with $\phi=2\pi/m$.

Thus, we choose

$$E_{zd}=A_m J_m(K_d r)\cos(m\phi)\, e^{-\gamma z} \qquad .....(3.2.1)^*$$

$$H_{zd}=B_m J_m(K_d r)\sin(m\phi)\, e^{-\gamma z} \qquad .....(3.2.2)^*$$

$$E_{zm}=C_m H_m^{(2)}(K_m r)\cos(m\phi)\, e^{-\gamma z} \qquad .....(3.2.3)^*$$

$$H_{zm}=D_m H_m^{(2)}(K_m r) \sin(m\phi) e^{-\gamma z}. \qquad .....(3.2.4)^*$$

From Maxwell's equations, the other field components can be obtained by substituting the above into the following[23]:

$$E_r=-\frac{1}{K^2}(\gamma\frac{\partial E_z}{\partial r}+\frac{j\omega\mu}{r}\frac{\partial H_z}{\partial \phi}) \qquad .....(3.2.5)$$

$$E_\phi=\frac{1}{K^2}(-\frac{\gamma}{r}\frac{\partial E_z}{\partial \phi}+j\omega\mu\frac{\partial H_z}{\partial r}) \qquad .....(3.2.6)$$

$$H_r=\frac{1}{K^2}(\frac{j\omega\varepsilon}{r}\frac{\partial E_z}{\partial \phi}-\gamma\frac{\partial H_z}{\partial r}) \qquad .....(3.2.7)$$

$$H_\phi=-\frac{1}{K^2}(j\omega\varepsilon\frac{\partial E_z}{\partial r}+\frac{\gamma}{r}\frac{\partial H_z}{\partial \phi}) \qquad .....(3.2.8)$$

which are obtained directly from Maxwell's equations by assuming the field components have the form

$$f(r,\phi)e^{-\gamma z} .$$

To satisfy these boundary conditions, we need to know, in addition to E_z and H_z, both E_ϕ and H_ϕ.

The azimuthal electric field intensity in the dielectric is,

$$E_{\phi d}=\frac{1}{K_d^2}(-\frac{\gamma}{r}[-mA_mJ_m(K_d r)\sin(m\phi)] + j\omega\mu_d K_d B_m J_m'(K_d r)\sin(m\phi))e^{-\gamma z}$$

or

$$E_{\phi d}=\frac{1}{K_d^2}(\frac{\gamma m}{r}A_mJ_m(K_d r)+j\omega\mu_d K_d B_m J_m'(K_d r))\sin(m\phi)\, e^{-\gamma z} .$$

The azimuthal electric field intensity in the metal is

$$E\phi_m = \frac{1}{K_m^2}\left(-\frac{\gamma}{r}\left[-mC_mH_m^{(2)}(K_mr)\right]\sin(m\phi)\right.$$

$$\left.+j\omega\mu_mK_mD_m\,H_m^{(2)\prime}(K_mr)\,\sin(m\phi)\right)e^{-\gamma z}$$

or

$$E\phi_m = \frac{1}{K_m^2}\left(\frac{\gamma m}{r}\,C_mH_m^{(2)}(K_mr)+j\omega\mu_mK_mD_m\,H_m^{(2)\prime}(K_mr)\sin(m\phi)\right)e^{-\gamma z}\ .$$

To calculate the magnetic field intensity in dielectric and metal, substitute E_{zd} and H_{zd} into (3.2.8) to get $H\phi_d$. In the same way, $H\phi_m$ can be easily obtained from E_{zm}, H_{zm} and (3.2.8).

Thus in the dielectric,

$$H\phi_d = -\frac{1}{K_d^2}\left(j\omega\varepsilon_dK_dA_mJ_m'(K_dr)\,\cos(m\phi)\right.$$

$$\left.+\frac{\gamma}{r}mB_mJ_m(K_dr)\,\cos(m\phi)\right)e^{-\gamma z}$$

or

$$H\phi_d = -\frac{1}{K_d^2}\left(j\omega\varepsilon_dK_dA_mJ_m'(K_dr)+\frac{\gamma}{r}mB_mJ_m(K_dr)\right)\cos(m\phi)\,e^{-\gamma z}\ .$$

In the metal,

$$H\phi_m = -\frac{1}{K_m^2}\left(j\omega\varepsilon_mK_mC_mH_m^{(2)\prime}(K_mr)\,\cos(m\phi)\right.$$

$$\left.+\frac{\gamma}{r}\,mD_mH_m^{(2)}(K_mr)\,\cos(m\phi)\right)e^{-\gamma z}$$

or

$$H\phi_m = -\frac{1}{K_m^2}\left(j\omega\varepsilon_m K_m C_m H_m^{(2)\prime}(K_m r) + \frac{\gamma}{r} m D_m H_m^{(2)}(K_m r)\right)\cos(m\phi)\, e^{-\gamma z} \ .$$

So far, by solving Maxwell's equations, the field components E_{zd}, H_{zd}, $E\phi_d$, $H\phi_d$ in the dielectric and E_{zm}, H_{zm}, $E\phi_m$, $H\phi_m$ in the metal are obtained. In the next step, the determinantal equation is derived from the matching of the electric and magnetic fields at the dielectric-metal interface .

At r=a $E_{zd}=E_{zm}$ yields

$$A_m J_m(K_d a) = C_m H_m^{(2)}(K_m a) \qquad .....(3.2.9)$$

$H_{zd}=H_{zm}$ yields

$$B_m J_m(K_d a) = D_m H_m^{(2)}(K_m a) \qquad .....(3.2.10)$$

$E\phi_d=E\phi_m$ yields

$$\frac{1}{K_d^2}\left(\frac{\gamma m}{a} A_m J_m(K_d a) + j\omega\mu_d K_d B_m J_m'(K_d a)\right)$$

$$= \frac{1}{K_m^2}\left(\frac{\gamma m}{a} C_m H_m^{(2)}(K_m a) + j\omega\mu_m K_m D_m H_m^{(2)\prime}(K_m a)\right) \ . \qquad .....(3.2.11)$$

Finally, $H\phi_d=H\phi_m$ yields

$$-\frac{1}{K_d^2}\left(j\omega\varepsilon_d K_d A_m J_m'(K_d a) + \frac{\gamma}{a} m B_m J_m(K_m a)\right)$$

$$= -\frac{1}{K_m^2}\left(j\omega\varepsilon_m K_m C_m H_m^{(2)\prime}(K_m a) + \frac{\gamma}{a} m D_m H_m^{(2)}(K_m a)\right) \ . \qquad .....(3.2.12)$$

We will construct the determinantal equation from (3.2.9-12).

First, solving for A_m, B_m, from (3.2.9) and (3.2.10) and substituting A_m and B_m into (3.2.11), we get the following:

$$\frac{\gamma m}{K_d^2 a}\,\frac{C_m H_m^{(2)}(K_m a)}{J_m(K_d a)}\,J_m(K_d a) + \frac{j\omega\mu_d}{K_d}\,\frac{D_m H_m^{(2)}(K_m a)}{J_m(K_d a)}\,J_m'(K_d a) = \frac{\gamma m}{K_m^2 a} C_m H_m^{(2)}(K_m a) + \frac{j\omega\mu_m}{K_m}\,D_m H_m^{(2)}{}'(K_m a)\ . \qquad .....(3.2.13)$$

A similar substitution of (3.2.9) and (3.2.10) into (3.2.12) obtains:

$$\frac{j\omega\varepsilon_d}{K_d}\,\frac{C_m H_m^{(2)}(K_m a)}{J_m(K_d a)}\,J_m'(K_d a) + \frac{\gamma m}{K_d^2 a}\,\frac{D_m H_m^{(2)}(K_m a)}{J_m(K_d a)}\,J_m(K_d a) = \frac{j\omega\varepsilon_m}{K_m}\,C_m H_m^{(2)}{}'(K_m a) + \frac{\gamma m}{K_m^2 a}\,D_m H_m^{(2)}(K_m a)\ . \qquad .....(3.2.14)$$

Rearranging (3.2.13), we obtain:

$$\frac{\gamma m}{a}\left(\frac{H_m^{(2)}(K_m a)}{K_d^2} - \frac{H_m^{(2)}(K_m a)}{K_m^2}\right) C_m + j\omega\left(\frac{\mu_d}{K_d}\,\frac{H_m^{(2)}(K_m a)}{J_m(K_d a)}\,J_m'(K_d a) - \frac{\mu_m}{K_m} H_m^{(2)}{}'(K_m a)\right) D_m = 0\ . \qquad .....(3.2.15)$$

Also, (3.2.14) can be written as :

$$-j\omega\left(\frac{\varepsilon_d}{K_d}\,H_m^{(2)}(K_m a)\,\frac{J_m'(K_d a)}{J_m(K_d a)}-\frac{\varepsilon_m}{K_m}\,H_m^{(2)\prime}(K_m a)\right)C_m$$

$$-\frac{\gamma m}{a}\left(\frac{H_m^{(2)}(K_m a)}{K_d^2}-\frac{H_m^{(2)}(K_m a)}{K_m^2}\right)D_m=0\ . \qquad \ldots\ldots(3.2.16)$$

For the last two equations to have non-trivial solutions for C_m and D_m , the determinant must be zero.

Setting the determinant to zero gives :

$$-\left(\frac{\gamma m}{a}\right)^2\left(H_m^{(2)}(K_m a)\right)^2\left(\frac{1}{K_d^2}-\frac{1}{K_m^2}\right)^2=$$

$$-\omega^2\left(\frac{\mu_d}{K_d}\,\frac{H_m^{(2)}(K_m a)}{J_m(K_d a)}J_m'(K_d a)-\frac{\mu_m}{K_m}\,H_m^{(2)\prime}(K_m a)\right)\times$$

$$\left(\frac{\varepsilon_d}{K_d}\,H_m^{(2)}(K_m a)\,\frac{J_m'(K_d a)}{J_m(K_d a)}-\frac{\varepsilon_m}{K_m}\,H_m^{(2)\prime}(K_m a)\right)\ .$$

$\ldots\ldots(3.2.17)$

The equation can be rewritten as:

$$\left(\frac{\mu_d}{K_d}\,\frac{J_m'(K_d a)}{J_m(K_d a)}-\frac{\mu_m}{K_m}\,\frac{H_m^{(2)\prime}(K_m a)}{H_m^{(2)}(K_m a)}\right)\times$$

$$\left(\frac{\varepsilon_d}{K_d}\,\frac{J_m'(K_d a)}{J_m(K_d a)}-\frac{\varepsilon_m}{K_m}\,\frac{H_m^{(2)\prime}(K_m a)}{H_m^{(2)}(K_m a)}\right)$$

$$=-\left(\frac{\gamma m}{\omega a}\right)^2\left(\frac{1}{K_d^2}-\frac{1}{K_m^2}\right)^2\ . \qquad \ldots\ldots(3.2.18)$$

Equation (3.2.18) is called the determinantal equation or characteristic equation, which must be solved for the propagation constant γ. The analysis of this thesis will be centered about this equation.

It should also be pointed out that this determinantal equation is valid for any two-medium cylindrical waveguides.

The characteristic equation gives the propagation characteristics of waveguides and this is very important in understanding the behavior of the fields. In the investigation of waveguides, one must solve or obtain an approximate solution of the determinantal equation to understand the field behavior.

3.3 Analysis of Perfect Conductor Waveguides

In order to have a greater understanding of the field problems we are dealing with, it is instructive to review the microwave case in which the metallic waveguide wall can be treated as a perfect conductor. Such a waveguide serves as a preliminary model for microstructural waveguides.

An important characteristic of good conductors is that the tangential components of the electric fields are close to zero at the surface of the conductor.

E_{zd}, H_{zd}, and $E\phi$ are rewritten here for reference:

$$E_{zd}=A_m J_m(K_d r) \cos(m\phi) e^{-\gamma z} \qquad .....(3.2.1)^*$$

$$H_{zd}=B_m J_m(K_d r) \sin(m\phi) e^{-\gamma z} \qquad .....(3.2.2)^*$$

$$E\phi = \frac{1}{K^2}\left(-\frac{\gamma}{r}\frac{\partial E_z}{\partial \phi} + j\omega\mu \frac{\partial H_z}{\partial r}\right) . \qquad .....(3.2.6)$$

Suppose now that neither A_m nor B_m are zero. Let us apply the boundary conditions. There are two arbitrary constants, so we use two conditions.

First, at r=a, E_z must vanish, since it is parallel to a perfect conductor. Thus from $(3.2.1)^*$,

$$J_m(K_d a)=0 .$$

Secondly, at r=a, $E\phi$ must vanish for the same reason. From (3.2.6) this requires,

$$\left(-\frac{\gamma}{r}\frac{\partial E_z}{\partial \phi} + j\omega\mu \frac{\partial H_z}{\partial r}\right) = 0 .$$

Since E_z and consequently $\frac{\partial E_z}{\partial \phi}$ vanishe at r=a, this reduces to :

$$\frac{\partial H_z}{\partial r} = 0$$

and so from $(3.2.2)^*$:

$$J_m'(K_d a)=0 .$$

Because $J_m'(K_d a)=0$ and $J_m(K_d a)=0$ can not be satisfied at the same time, we have to choose one of A_m, B_m to be zero at a time.

If we select $A_m= 0$, then from the above argument

$$J_m'(K_d a)=0 \ .$$

In this case the electric fields are on the transverse plane only, and we have a TE mode.

If we select $B_m = 0$, then

$$J_m(K_d a)=0 \ .$$

In this case the magnetic fields lie in the transverse plane only, and we have a TM mode.

It follows that we have only two kinds of modes, TE modes and TM modes.

For a waveguide wall consisting of a good but not perfect conductor, we have that:

$J_m(K_d a) \longrightarrow 0$ for TM modes

and $J_m'(K_d a) \longrightarrow 0$ for TE modes .

In this case the determinantal equation can be solved by perturbing $J_m(K_d a)$ or $J_m'(K_d a)$ respectively about their zeros, that is, expanding $J_m(K_d a)$ or $J_m'(K_d a)$ in a Taylor series expansion about values of their arguments which are roots of these functions. We will discuss this in detail later.

It should be mentioned here that, for circular cross-section waveguides, $J_m(K_d a) = 0$ or $J_m'(K_d a) = 0$ holds only for perfect conductor waveguides. No great significance should be attached to this fact. It should not be allowed to color our ideas about waveguides in general. We will come back to this point in Chapter 4.

4 ANALYTICAL RESULTS FOR CYLINDRICAL MICROSTRUCTURAL WAVEGUIDES

4.1 General Comments

Although the transmission characteristics of cylindrical metallic waveguides are well-known at microwave frequencies, the theory is invalidated and therefore must be altered for operation at optical wavelengths in a micron-sized waveguide of circular cross section. For the latter, the metal no longer acts as a good conductor, but rather as a dielectric having a complex dielectric constant. In the subsequent analysis, therefore, we consider a hollow circular waveguide having an external medium made of an evaporated gold film whose optical properties are characterized by a finite complex refractive index.

To solve the radiation transmission problem in hollow gold-coated waveguides of circular cross section, we have several alternatives: first, because the reflectance of a gold film is very high for infrared radiation, it seems to be possible to perturb the perfect conductor boundary conditions. i.e. to perturb $J_m(Kda)$ or $J_m'(Kda)$, respectively, in the determinantal equation(3.2.18).

However, we will show that in cylindrical microstructural waveguides, the assumptions that the tangential E-field at the boundary is small and consequently that $J_m(Kda) \longrightarrow 0$ or $J_m'(Kda) \longrightarrow 0$ could lead us to

contradictions in some cases. In those cases, perturbation of $J_m(K_da)$ or $J_m'(K_da)$ is physically unrealistic and does not provide solutions to the characteristic equation.

The essence of the perturbation calculation is to determine a small change in the propagation constant of the electromagnetic field in a loss-free waveguide, due to a small departure of the physical system from the loss-free model used. Thus the perturbation method depends on the unperturbed model. This is the limitation of the method.

The second alternative is that we may use the power flow method, which is explained below in more detail.

Because of the imperfectly conducting waveguide walls, the electric and magnetic fields propagating along the waveguide will posses an attenuation factor $e^{-\alpha z}$. The field magnitudes can be written as

$$|E| = |Eo|e^{-\alpha z}$$

$$|H| = |Ho|e^{-\alpha z}$$

where Ho and Eo are the intensities at z=0.
Thus the time-average power transmitted through the waveguide is expressed by

$$W_T = Wo\ e^{-2\alpha z}\ .$$

where $Wo = \int_{A2} \frac{1}{2} Re(E_o \times H_o^*) \cdot da$; the integration is over the cross section of the waveguide.

The power loss per unit length of waveguide is the

spatial rate of decrease of power transmitted, i.e.

$$W_L = - \frac{\partial W_T}{\partial z} = 2\alpha W_T \ .$$

Hence, we obtain the desired relationship for the attenuation constant:

$$\alpha = \frac{W_L}{2W_T} \ .$$

The problem is that in many cases of interest it may be difficult to calculate W_L and W_T. To calculate these quantities, we have to know the electric and magnetic field distributions. However, the electric fields and magnetic fields are determined by the unknown attenuation constant α.

If we assume the guide walls are perfectly conducting or that at least we can apply the boundary condition that the tangential component of electric field is close to zero, then the distributions of electric and magnetic field intensities in the interior of the guide or on the guide walls are, except for attenuation in the direction of propagation, essentially those that exist in a loss-free guide. Therefore, from Poynting's theorem and the tangential magnetic field intensity, the power flowing into the guide walls may be calculated. Since we can also calculate W_T, it is possible to calculate the attenuation constant.

However, this method is only valid for those perfect conductor waveguides or waveguides with modes whose boundary conditions are such that the tangential components of electric fields are close to zero. The method is not

universally applicable.

From the above discussion it is clear that it might be possible to use the perturbation method and the power flow method to derive the propagation characteristics of circular microstructural guides, but we have to use these methods with some discretion. As a matter of fact, these methods should not be applied without analyzing the determinantal(characteristic) equation first. Because the determinantal equation contains all the information about the characteristics of wave propagation in waveguides, we can not set aside the determinantal equation and make our own assumptions about the fields within the guide or at the guide boundaries.

The assumptions $J_m(Ka) \longrightarrow 0$ or $J_m'(Ka) \longrightarrow 0$ can not be made *a priori*. However the determinantal equation itself can tell us if these assumptions are really correct. By use of the determinantal equation we will show that for TE modes in microstructural cylindrical waveguides, $J_m'(Ka) \longrightarrow 0$, which implies also that $E\phi \cong 0$. Hence for TE modes, the perturbation and power flow methods may be used to calculate the attenuation constant α. Calculation of the attenuation constant α for TM modes and hybrid modes is more difficult and will be investigated later in this thesis.

4.2 Designation of Modes

Because hollow microstructural waveguides are completely new devices to be analyzed for the first time for cylindrical systems in this thesis, any ideas and techniques from the microwave frequency waveguides or optical waveguides of large dimensions should not be accepted without questioning. As it will be shown later some ideas are still applicable to our microstructural guides, but we have to prove this by analyzing the determinantal equation, which, as mentioned above, contains all the information about the electromagnetic fields in the waveguides. We can not even take the existence of TE modes or TM modes for granted. Fortunately they do exist in our case, under some special circumstances.

As a matter of fact, in a cylindrical guiding structure, it turns out that a TE or TM mode is possible only if either:

(1) the outer surface is a perfect conductor;

(2) the field solution has no ϕ dependence, i.e it has cylindrical symmetry.

For all other cases, in particular for our gold-coated microstructural waveguides, both an axial E and H must be present so that it is possible to satisfy all boundary conditions. The field solutions in those cases consist of a superposition of TM and TE modes in both the loss-free dielectric region and the metal region.

From the determinantal equation (3.2.18)

$$\left(\frac{\mu_d J_m'(K_d a)}{K_d J_m(K_d a)} - \frac{\mu_m H_m^{(2)}{}'(K_m a)}{K_m H_m^{(2)}(K_m a)}\right)\left(\frac{\varepsilon_d J_m'(K_d a)}{K_d J_m(K_d a)} - \frac{\varepsilon_m H_m^{(2)}{}'(K_m a)}{K_m H_m^{(2)}(K_m a)}\right)$$

$$= -\left(\frac{\gamma m}{\omega a}\right)^2 \left(\frac{1}{K_d^2} - \frac{1}{K_m^2}\right)^2 .$$

We have, if m=0,

$$\frac{\mu_d J_o'(K_d a)}{K_d J_o(K_d a)} - \frac{\mu_m H_o^{(2)}{}'(K_m a)}{K_m H_o^{(2)}(K_m a)} = 0 \qquad .....(4.2.1)$$

Or

$$\frac{\varepsilon_d J_o'(K_d a)}{K_d J_o(K_d a)} - \frac{\varepsilon_m H_o^{(2)}{}'(K_m a)}{K_m H_o^{(2)}(K_m a)} = 0 \qquad .....(4.2.2)$$

We will now prove that (4.2.1) implies $E_z=0$.

We rewrite (3.2.11), (3.2.9), (3.2.10)

$$\frac{1}{K_d^2}\left(\frac{\gamma m}{a} A_m J_m(K_d a) + j\omega\mu_d K_d B_m J_m'(K_d a)\right)$$

$$= \frac{1}{K_m^2}\left(\frac{\gamma m}{a} C_m H_m^{(2)}(K_m a) + j\omega\mu_m K_m D_m H_m^{(2)}{}'(K_m a)\right)$$

$$.....(3.2.11)$$

$$A_m J_m(K_d a) = C_m H_m^{(2)}(K_m a) \qquad .....(3.2.9)$$

$$B_m J_m(K_m a) = D_m H_m^{(2)}(K_m a) \qquad .....(3.2.10)$$

Equation (3.2.11) can be changed to,

$$\frac{1}{K_d^2}\left(\frac{\gamma m}{a} A_m J_m(K_d a) + j\omega\mu_d K_d B_m J_m'(K_d a)\right)$$

$$= \frac{1}{K_m^2}\left(\frac{\gamma m}{a} A_m J_m(K_d a) + j\omega\mu_m K_m D_m H_m^{(2)}{}'(K_m a)\right)$$

Dividing both sides by B_m,

$$\frac{1}{K_d^2}\left(\frac{\gamma m}{a}\frac{A_m}{B_m}J_m(K_d a)+j\omega\mu_d K_d J_m'(K_d a)\right)$$

$$=\frac{1}{K_m^2}\left(\frac{\gamma m}{a}\frac{A_m}{B_m}J_m(K_d a)+j\omega\mu_m K_m\frac{D_m}{B_m}H_m^{(2)}'(K_m a)\right)$$

From (3.2.10), we obtain,

$$\frac{D_m}{B_m}=\frac{J_m(K_d a)}{H_m^{(2)}(K_m a)}$$

Hence we have ,

$$\frac{1}{K_d^2}\left(\frac{\gamma m}{a}\frac{A_m}{B_m}J_m(K_d a)+j\omega\mu_d K_d J_m'(K_d a)\right)$$

$$=\frac{1}{K_m^2}\left(\frac{\gamma m}{a}\frac{A_m}{B_m}J_m(K_d a)+j\omega\mu_m K_m\frac{J_m(K_d a)}{H_m^{(2)}(K_m a)}H_m^{(2)}'(K_m a)\right)$$

Dividing both sides by $J_m(K_d a)$,

$$\frac{1}{K_d^2}\left(\frac{\gamma m}{a}\frac{A_m}{B_m}+j\omega\mu_d K_d\frac{J_m'(K_d a)}{J_m(K_d a)}\right)$$

$$=\frac{1}{K_m^2}\left(\frac{\gamma m}{a}\frac{A_m}{B_m}+j\omega\mu_m K_m\frac{H_m^{(2)}'(K_m a)}{H_m^{(2)}(K_m a)}\right)$$

Therefore,

$$\frac{\gamma m}{a}\frac{A_m}{B_m}\left(\frac{1}{K_m^2}-\frac{1}{K_d^2}\right)=j\omega\left(\frac{\mu_d}{K_d}\frac{J_m'(K_d a)}{J_m(K_d a)}-\frac{\mu_m}{K_m}\frac{H_m^{(2)}'(K_m a)}{H_m^{(2)}(K_m a)}\right)$$

It follows that,

$$\frac{A_m}{B_m}=\frac{a}{\gamma m}\left(\frac{1}{K_m^2}-\frac{1}{K_d^2}\right)^{-1}j\omega\left(\frac{\mu_d}{K_d}\frac{J_m'(K_d a)}{J_m(K_d a)}-\frac{\mu_m}{K_m}\frac{H_m^{(2)}'(K_m a)}{H_m^{(2)}(K_m a)}\right)$$

From (3.2.18),

$$\left(\frac{\mu_d}{K_d}\frac{J_m'(K_d a)}{J_m(K_d a)} - \frac{\mu_m}{K_m}\frac{H_m^{(2)\prime}(K_m a)}{H_m^{(2)}(K_m a)}\right)\times$$

$$\left(\frac{\varepsilon_d}{K_d}\frac{J_m'(K_d a)}{J_m(K_d a)} - \frac{\varepsilon_m}{K_m}\frac{H_m^{(2)\prime}(K_m a)}{H_m^{(2)}(K_m a)}\right)$$

$$= -\left(\frac{\gamma m}{\omega a}\right)^2\left(\frac{1}{K_d^2} - \frac{1}{K_m^2}\right)^2$$

We can express m as,

$$m = \frac{j\omega a}{\gamma}\left(\frac{\mu_d}{K_d}\frac{J_m'(K_d a)}{J_m(K_d a)} - \frac{\mu_m}{K_m}\frac{H_m^{(2)\prime}(K_m a)}{H_m^{(2)}(K_m a)}\right)^{1/2}\times$$

$$\left(\frac{\varepsilon_d}{K_d}\frac{J_m'(K_d a)}{J_m(K_d a)} - \frac{\varepsilon_m}{K_m}\frac{H_m^{(2)\prime}(K_m a)}{H_m^{(2)}(K_m a)}\right)^{1/2} \Big/ \left(\frac{1}{K_d^2} - \frac{1}{K_m^2}\right)$$

Then we have,

$$\frac{A_m}{B_m} = \frac{\left(\frac{\mu_d}{K_d}\frac{J_m'(K_d a)}{J_m(K_d a)} - \frac{\mu_m}{K_m}\frac{H_m^{(2)\prime}(K_m a)}{H_m^{(2)}(K_m a)}\right)^{1/2}}{\left(\frac{\varepsilon_d}{K_d}\frac{J_m'(K_d a)}{J_m(K_d a)} - \frac{\varepsilon_m}{K_m}\frac{H_m^{(2)\prime}(K_m a)}{H_m^{(2)}(K_m a)}\right)^{1/2}} \quad \text{.....(4.2.3)}$$

When (4.2.1) is applied for m=0, the numerator in the right hand side of (4.2.3) becomes zero, and therefore we have,

$$A_m = 0$$

From (3.2.1), this implies $E_{zd}=0$. Thus the electric field is transverse to the axial direction. We call this a TE mode.

Equation (4.2.3) can be written as,

$$\frac{B_m}{A_m} = \frac{\left(\frac{\varepsilon_d}{K_d}\,\frac{J_m'(K_d a)}{J_m(K_d a)} - \frac{\varepsilon_m}{K_m}\,\frac{H_m^{(2)\prime}(K_m a)}{H_m^{(2)}(K_m a)}\right)^{1/2}}{\left(\frac{\mu_d}{K_d}\,\frac{J_m'(K_d a)}{J_m(K_d a)} - \frac{\mu_m}{K_m}\,\frac{H_m^{(2)\prime}(K_m a)}{H_m^{(2)}(K_m a)}\right)^{1/2}} \qquad .....(4.2.4)$$

When (4.2.2) is used for m=0, we have $B_m=0$ which, from (3.2.2), in turn means $H_z=0$. That is, the magnetic field is transverse to the axial direction; it is a TM mode.

Therefore, (4.2.1) is the determinantal equation for TE modes and (4.2.2) is the determinantal equation for TM modes.

If $m\neq 0$, neither A_m nor $B_m=0$, so that both H_z and E_z have non-zero values. These modes are called hybrid modes.

Note that (4.2.1) and (4.2.2) can not hold at the same time by solving (4.2.1) and (4.2.2) respectively for $\frac{J_o'(K_d a)}{J_o(K_d a)}$: since $\varepsilon_m/\varepsilon_d \gg 1$, the two expressions for $\frac{J_o'(K_d a)}{J_o(K_d a)}$ can never have the same value.

4.3 Simplification of Determinantal Equation

The attenuation constant for cylindrical waveguides will be derived by a direct solution of the determinantal equation.

Equation (3.2.18) is the determinantal equation for

cylindrical microstructural waveguides, where

$$K_d^2 = \omega^2\mu_d\varepsilon_d + \gamma^2, \quad K_m^2 = \omega^2\mu_m\varepsilon_m + \gamma^2, \quad \gamma = \alpha + j\beta$$

and the complex permittivity is $\varepsilon_m = \varepsilon' - j\varepsilon''$. Hence, for non-magnetic materials, $\mu_m = \mu_d = \mu_o$, and so we have:

$$K_m^2 = \omega^2\mu_m\varepsilon_m + \gamma^2 = \frac{\varepsilon_m}{\varepsilon_d}\,\omega^2\mu_m\varepsilon_d + \gamma^2 = \frac{\varepsilon_m}{\varepsilon_d}\,\omega^2\mu_d\varepsilon_d + \gamma^2$$

From [22], inside the gold film:

$$K_m^2 \cong \omega^2\mu_m\varepsilon_m$$

This approximation is proved as follows.

For a moderately lossy waveguide, the real part of γ (attenuation constant) is much smaller than the its imaginary part (phase constant). Also when losses are small,the phase constant of a lossy guide is approximately the same as that of loss-free counterpart.

For the loss-free guide,

$$\gamma^2 \cong \omega^2\mu_o\varepsilon_o\left(1-\left(\frac{f_c}{f}\right)^2\right)^{1/2}$$

where f is the frequency at which the waveguide is operated and f_c is the cutoff frequency. The cutoff frequency is discussed in more detail in Section 4.4.

Since $K_m^2 = \gamma^2 + \omega^2\mu_m\varepsilon_m \cong \omega^2\mu_o\varepsilon_o\left(1-\left(\frac{f_c}{f}\right)^2\right)^{1/2} + \omega^2\mu_m\varepsilon_m$

and for typical operation of a guide f is generally larger

than $2f_c$, then $K_m^2 \cong \omega^2\mu_o\varepsilon_o + \omega^2\mu_m\varepsilon_m$.

Comparing the two terms in the approximate expression of K_m^2, we find that $\omega^2\mu_m\varepsilon_m \gg \omega^2\mu_o\varepsilon_o$, because $\varepsilon_m \gg \varepsilon_d$, as mentioned in Section 3.1.

Hence, $$K_m^2 \cong \omega^2\mu_m\varepsilon_m$$

or $$K_m \cong \omega\sqrt{\mu_m\varepsilon_m}$$

$$K_m \cong \omega\sqrt{\mu_o\varepsilon_o}\ \sqrt{\varepsilon_m/\varepsilon_o}$$

Since

$$\omega\sqrt{\mu_o\varepsilon_o} \equiv \frac{2\pi}{\lambda_o}$$

and $$\sqrt{\varepsilon_m/\varepsilon_o} = N = n\text{-}jk \ .$$

We have that

$$K_m a \cong \frac{2\pi a}{\lambda_o}\ (n\text{-}jk) \ .$$

In this thesis we examine microstructural waveguides for which the ratio a/λ_o ranges from 1 to 20. Cases for which $a/\lambda_o > 20$ are excluded from this study. On the other hand if $a/\lambda_o < 1$, the losses become prohibitively large and will also not be considered. .

The approximate size of $K_m a$ is easily evaluated. At 1.033μm when $n\text{-}jk=0.272\text{-}j7.07$(TABLE I) and for $a/\lambda_o=1$, $|K_m a|$ is about 42. This corresponds to the smallest value of $K_m a$

encountered in the present research(see values of n and k in TABLE I used to calculate $|K_{ma}|$).

It follows therefore that: $|K_{ma}| \gg 1$

Thus the magnitude of the argument of the Hankel function of the second kind is much larger than one, and we can apply to the determinantal equation the asymptotic behavior of the Hankel function for large arguments, namely

$$\frac{H_m^{(2)\prime}(K_{ma})}{H_m^{(2)}(K_{ma})} \longrightarrow -j$$

This result follows from the identity[27], [28]:

$$x\, H_m^{(2)\prime}(x) \equiv mH_m^{(2)}(x) - (x)H_{m+1}^{(2)}(x)$$

which leads to

$$\frac{H_m^{(2)\prime}(x)}{H_m^{(2)}(x)} = \frac{m}{x} - \frac{H_{m+1}^{(2)}(x)}{H_m^{(2)}(x)}$$

From [23], for sufficiently large x,

$$H_m^{(2)}(x) \cong \sqrt{2/\pi x}\; e^{-j[x-\pi/4-m\pi/2]}$$

$$H_{m+1}^{(2)}(x) \cong \sqrt{2/\pi x}\; e^{-j[x-\pi/4-(m+1)\pi/2]}$$

Thus

$$\frac{H_m^{(2)\prime}(x)}{H_m^{(2)}(x)} \cong \frac{m}{x} - \frac{e^{j(m+1)\pi/2}}{e^{jm\pi/2}} = \frac{m}{x} - e^{j\pi/2}$$

Therefore,

$$\frac{H_m^{(2)\prime}(x)}{H_m^{(2)}(x)} \cong \frac{m}{x} - j$$

Thus for $K_m a$ sufficiently large in relation to m,

$$\frac{H_m^{(2)\prime}(K_m a)}{H_m^{(2)}(K_m a)} \cong -j.$$

Validity of this approximation for our research will be discussed in Chapter 5.

Hence the determinantal equation(3.2.18) then simplifies to :

$$\left(\frac{\mu_d J_m'(K_d a)}{K_d J_m(K_d a)} + \frac{\mu_m}{K_m} j \right) \left(\frac{\varepsilon_d J_m'(K_d a)}{K_d J_m(K_d a)} + \frac{\varepsilon_m}{K_m} j \right)$$

$$= -\left(\frac{\gamma m}{\omega a}\right)^2 \left(\frac{1}{K_m^2} - \frac{1}{K_d^2} \right)^2 \qquad .....(4.3.1)$$

Similarly, from (4.2.1) the simplified determinantal equation for TE modes is

$$\frac{\mu_d J_o'(K_d a)}{K_d J_o(K_d a)} + \frac{\mu_m}{K_m} j = 0 \qquad .....(4.3.2)$$

and from (4.2.2), the determinantal equation for TM modes simplifies to

$$\frac{\varepsilon_d J_o'(K_d a)}{K_d J_o(K_d a)} + \frac{\varepsilon_m}{K_m} j = 0 \qquad .....(4.3.3)$$

We will discuss the asymptotic behavior of Hankel functions in more detail in Chapter 5.

4.4 Characteristics of TE Modes

We shall derive here an approximate expression for the attenuation constant α of TE modes for which m=0, and which are therefore cylindrically symmetric. The approximate expression for α is obtained from the determinantal equation. Having done this, we shall then take the limiting case of the expression that has been obtained for α as n and k are selected to be representative of a perfect conductor. This limiting value of α will then be shown to be identical to that of a metallic waveguide at microwave frequencies.

Having done this, we then evaluate the approximate attenuation constant α for a gold-coated microstructural waveguide a second way, using the power flow method.

From (4.3.2), the determinantal equation for TE modes for a non-magnetic material is:

$$\frac{J_o'(K_d a)}{J_o(K_d a)} = -j\frac{K_d}{K_m}$$

Because of the relation derived in Section 4.3, namely,

$$K_m a \cong \frac{2\pi a}{\lambda_o}\ (n-jk)$$

the determinantal equation becomes:

$$\frac{J_o'(K_d a)}{(K_d a)J_o(K_d a)} = -j\frac{\lambda_o}{2\pi a}\ \frac{1}{(n-jk)} \qquad .....(4.4.1)$$

We can see that if $a/\lambda_o=1$ and $\lambda_o=1.033\mu m$ the value of the magnitude of the right hand side of (4.4.1) is roughly 1/42, which is much smaller than 1. As λ_o is in the range $1\mu m$-$10\mu m$ and a/λ_o is from 1 to 20 for this research, 1/42 is the largest value for the magnitude of the right hand side of (4.4.1). Thus the determinantal equation itself shows us that the left hand side of (4.4.1) will be very small, which means that $J_o'(K_da)$ is very small. In other words, it is consistent with the determinantal equation that $J_o'(K_da)\longrightarrow 0$. Physically this means that the tangential electric field $E\phi$ of TE modes at the boundary is close to zero.

Since $J_o'(K_da)\longrightarrow 0$, we have $K_da \cong p'_n$, where p'_n is the n-th root of $J_o'(x)=0$. Therefore by analogy with the lossless waveguides, the TE modes can be denoted as TE_{on} modes.

From the identity, $J_o'(x)=-J_1(x)$, we can rewrite the determinantal equation (4.4.1) as:

$$-\frac{J_1(K_da)}{J_o(K_da)}=-j(K_da)\frac{\lambda_o}{2\pi a}\frac{1}{(n-jk)} \qquad .....(4.4.2)$$

We will find an approximate solution to this equation for TE modes.

As mentioned above, for TE modes, $E\phi$ goes to zero at r=a. This follows since $J_o'(K_da)\longrightarrow 0$, or equivalently $J_1(K_da)\longrightarrow 0$. Thus $J_1(K_da)$ on the left-hand side of (4.4.2)

can be expanded around the point p_{1n}, where p_{1n} is the nth root of $J_1(x)=0$.

Performing a Taylor series expansion and retaining only the first two terms,

$$J_1(K_d a) \cong J_1(p_{1n}) + (K_d a - p_{1n}) J_1'(x)\Big|_{x=p_{1n}}$$

Taking into consideration the identities

$$J_1'(x) \equiv J_0(x) - \frac{1}{p_{1n}} J_1(x) \qquad J_1(x) \equiv -J_0'(x)$$

we obtain $J_1(K_d a) \cong (K_d a - p_{1n}) J_0(p_{1n})$. Now take this together with $J_0(K_d a) \cong J_0(p_{1n})$, and (4.4.2) becomes

$$K_d a - p_{1n} \cong j(K_d a) \frac{\lambda_0}{2\pi a} \frac{1}{(n-jk)}$$

Hence $K_d \cong \frac{p_{1n}}{a} \left(1/\left(1-j\frac{\lambda_0}{2\pi a} \frac{1}{n-jk}\right)\right)$

Since $\left|j\frac{\lambda_0}{2\pi a} \frac{1}{n-jk}\right| \ll 1$ and $\frac{1}{1-x} \cong 1+x$ for $|x| \ll 1$,

therefore, $K_d^2 \cong \left(\frac{p_{1n}}{a}\right)^2 \left(1+j\frac{\lambda_0}{2\pi a} \frac{1}{(n-jk)}\right)^2$

Now $(1+x)^2 \cong 1+2x$ for $|x| \ll 1$

Thus,

$$K_d^2 \cong \left(\frac{p_{1n}}{a}\right)^2\left(1+2j\frac{\lambda_o}{2\pi a}\ \frac{1}{(n-jk)}\right)$$

Since $\gamma^2 = -k^2 + K_d^2$ and $k^2=\left(\frac{2\pi}{\lambda_o}\right)^2$

hence $\gamma^2=-k^2+ k^2\left(\frac{p_{1n}}{a}\right)^2\left(1+2j\frac{\lambda_o}{2\pi a}\ \frac{1}{(n-jk)}\right)\left(\frac{\lambda_o}{2\pi}\right)^2$

Thus, $\gamma^2= -k^2\left(1-\left(\frac{p_{1n}\lambda_o}{2\pi a}\right)^2\left(1+2j\frac{\lambda_o}{2\pi a}\ \frac{1}{(n-jk)}\right)\right)$

or ,

$$\gamma^2= -k^2\left(\left(1-\left(\frac{p_{1n}\lambda_o}{2\pi a}\right)^2\right) - \left(\frac{p_{1n}\lambda_o}{2\pi a}\right)^2\ 2j\frac{\lambda_o}{2\pi a}\ \frac{1}{(n-jk)}\right)$$

Therefore, taking the square root of both sides of the above equation it can be seen that:

$$\gamma = jk\left(\left(1-\left(\frac{p_{1n}\lambda_o}{2\pi a}\right)^2\right) - \left(\frac{p_{1n}\lambda_o}{2\pi a}\right)^2\ 2j\frac{\lambda_o}{2\pi a}\ \frac{1}{(n-jk)}\right)^{1/2} \ldots\ldots (4.4.3)$$

In a perfect-conductor waveguide, there is a cut-off frequency. Below that frequency, the waves interfere destructively and vanish after a very short distance. Above that frequency, the waves are transmitted without any losses.

It is quite different for a non-perfect-conducting waveguide. In such a waveguide, there are losses at all frequencies. Thus, a distinct cutoff does not occur. But the concept of the cutoff frequency is still useful for

non-perfect-conductor waveguides. For the latter the cutoff frequency is the frequency below which losses are very large and above which they are relatively small.

For TE modes in a loss-free perfectly conducting waveguide, the cutoff wavelength[23] is $\lambda_c=\frac{2\pi a}{p_{1n}}$. The corresponding cutoff frequency is $f_c=1/\lambda_c\sqrt{\mu_o\varepsilon_o}$.

Hence, when $f \geq 1.5f_c$, which defines the typical operating range for f in a waveguide system, $\lambda_c \geq 1.5\lambda_o$ and we can obtain the following:

$$\frac{p_{1n}\lambda_o}{2\pi a} \leq \frac{2}{3}$$

From the above inequality, it follows that

$$\left|1-\left(\frac{p_{1n}\lambda_o}{2\pi a}\right)^2\right| \gg \left|-\left(\frac{p_{1n}\lambda_o}{2\pi a}\right)^2 2j\frac{\lambda_o}{2\pi a}\frac{1}{(n-jk)}\right|$$

and since $(x-y)^{1/2} \cong x^{1/2} - \frac{1}{2}x^{-1/2}y$, for $|x| \gg |y|$,

(4.4.3) can be written as :

$$\gamma \cong jk\left[\left(1-\left(\frac{p_{1n}\lambda_o}{2\pi a}\right)^2\right)^{1/2} - \frac{1}{2}\left(1-\left(\frac{p_{1n}\lambda_o}{2\pi a}\right)^2\right)^{-1/2}\left(\left(\frac{p_{1n}\lambda_o}{2\pi a}\right)^2 \quad 2j\frac{\lambda_o}{2\pi a} \quad \frac{1}{(n-jk)}\right)\right]$$

The attenuation constant α for TE modes with m=0 in gold-coated microstructural waveguides is obtained from the above by equating real and imaginary parts in $\gamma=\alpha+j\beta$

$$\alpha = \frac{1}{a}\frac{n}{n^2+k^2}\left(\left(\frac{p_{1n}\lambda_o}{2\pi a}\right)^2 \Big/ \sqrt{1-\left(\frac{p_{1n}\lambda_o}{2\pi a}\right)^2}\right) \quad \ldots\ldots \quad (4.4.4)$$

We can now show that this result agrees in the limiting case with the attenuation constant α for TE modes in a metallic waveguide in the microwave region. In this region[23],

$$\alpha = \frac{R_s}{a\eta_o}\frac{1}{f^2}\left(1/\left(1-\frac{f_c^2}{f^2}\right)^{1/2}\right) \quad .....(4.4.5)$$

where the intrinsic impedance is $\eta_o=\left(\frac{\mu_o}{\varepsilon_o}\right)^{1/2}$, and the surface resistivity is $R_s = \left(\frac{\pi f\mu_o}{\sigma}\right)^{1/2}$,

Since $\varepsilon''/\varepsilon_o = 2nk$, and $\sigma=\omega\varepsilon''$, as mentioned in Chapter 3, it follows that $2nk = \frac{\sigma}{\varepsilon_o\omega}$,

For a good conductor, since $\sigma \longrightarrow \infty$ we have,

$$N=n-jk= \sqrt{\varepsilon_m/\varepsilon_o}= \left(\frac{\varepsilon'-j\varepsilon''}{\varepsilon_o}\right)^{1/2} = \left(\frac{\varepsilon'}{\varepsilon_o} -j\frac{\sigma}{\varepsilon_o\omega}\right)^{1/2}$$

$$n-jk \cong \left(-j\frac{\sigma}{\varepsilon_o\omega}\right)^{1/2} = \left(\frac{\sigma}{2\varepsilon_o\omega}\right)^{1/2}(1-j)$$

It follows that $n=k$ and $n^2=\frac{\sigma}{2\varepsilon_o\omega}$

Therefore $\frac{n}{n^2+k^2} = \frac{n}{2n^2} = \frac{1}{2n} = \left(\frac{\varepsilon_o\omega}{2\sigma}\right)^{1/2}$

But $\left(\frac{\varepsilon_o\omega}{2\sigma}\right)^{1/2} = \left(\frac{\varepsilon_o\pi f}{\sigma}\right)^{1/2} = \left(\frac{\varepsilon_o}{\mu_o}\right)^{1/2}\left(\frac{\pi f\mu_o}{\sigma}\right)^{1/2} = \frac{R_s}{\eta}$

also, since $\lambda_c = \frac{2\pi a}{p_{1n}}$, $f_c = 1/\lambda_c\sqrt{\mu_o\varepsilon_o}$.

and hence in (4.4.4) $\left(\frac{p_{1n}\lambda_o}{2\pi a}\right)^2=\left(\frac{\lambda_o}{\lambda_c}\right)^2=\left(\frac{f_c}{f}\right)^2$

It can be easily seen that in the limit as the walls of the guide become perfectly conducting, the approximate attenuation constant (4.4.4) has exactly the same form as the attenuation constant at microwave frequencies, given in (4.4.5).

We will now use the power flow method to derive the attenuation constant. While this approach for finding α is conceptually different from the approach using the determinantal equation, the end result is shown to be the same. As shown in Section 4.1,

$$\alpha = \frac{W_L}{2W_T}$$

To evaluate the losses due to the imperfect waveguide walls, we at first try to obtain the electric fields and magnetic fields in a perfectly conducting guide. As mentioned above the circumferential electric field intensity $E\phi$ at the boundary is very close to zero. However there will be a tangential axial magnetic field intensity on the boundary of the waveguides. Therefore, we may evaluate the power dissipated per unit length of surface in the waveguide walls by using Poynting's theorem. The power loss per unit length of guide is obtained by integrating the power density

over the surface of the boundary corresponding to unit length of waveguide.

Thus $W_L = \oint_s \left(\frac{1}{2}\mathrm{Re}(\mathbf{E}\times\mathbf{H}^*)\right)\cdot d\mathbf{S}$

where $\oint_s dS$ denotes the integration over the surface of the waveguide of one meter length in the z-direction.

For TE modes we express the above as:

$$W_L = \frac{1}{2}\oint_s \mathrm{Re}(E\phi \times H_z^*)\cdot dS$$

but since $\eta_m = \frac{E\phi}{H_z}$ and $\nabla\times\mathbf{E} = -j\omega\mu\mathbf{H}$

$$\eta_m = \frac{E\phi}{H_z} = j\omega\mu/\gamma_m \ , \quad \text{here } \gamma_m = j\omega\sqrt{\mu_m\varepsilon_m}$$

$$\eta_m = \sqrt{\mu_m/\varepsilon_m}$$

then $W_L = \frac{1}{2}\oint_s \mathrm{Re}(\eta_m H_z\cdot H_z^*)dS = \frac{1}{2}\mathrm{Re}(\eta_m)\oint_s |H_z|^2 dS$

For non-magnetic materials,

$$\eta_m = \sqrt{\mu_m/\varepsilon_m} = \sqrt{\mu_o/\varepsilon_o}\cdot\sqrt{\varepsilon_o/\varepsilon_m} = \eta_o\frac{1}{(n-jk)}$$

and hence, $\mathrm{Re}(\eta_m) = \eta_o\frac{n}{n^2+k^2}$

Because $H_z = H_o J_o(Kda)$, for TE modes,

from [23], the integral $\oint_s |H_z|^2 dS = 2a\pi H_o^2 J_o^2(Kda)$

and hence $W_L = \frac{1}{2}\eta_o\frac{n}{n^2+k^2}\,2a\pi H_o^2 J_o^2(Kda)$

Next, the power transferred is,

$$W_T = \int_A \frac{1}{2}\mathrm{Re}(\mathbf{E}\times\mathbf{H}^*)\cdot da,$$

where $\int_A da$ is the integration over the cross section of

the waveguide. Since the fields we are using are those for loss-free propagation, this integral is identical to the usual integral for power flow at microwave frequencies in a perfectly conducting waveguide. It is given by [23].

$$W_T = \frac{\pi a^2}{4} \eta_o \left(\frac{\lambda_c}{\lambda_o}\right)^2 \left[1-\left(\frac{\lambda_o}{\lambda_c}\right)^2\right]^{1/2} H_o^2 J_o^2(K_d a)$$

If we substitute W_T and W_L into $\alpha = W_L/2W_T$, then we obtain an expression for α which is exactly the same as the formula for α obtained earlier in (4.4.4), using the determinantal equation as a starting point.

4.5 Characteristics of TM Modes

In this section, we wish to show that for TM modes of microstructural cylindrical waveguides, unlike their microwave counterparts, $J_o(K_d a)$ can <u>not</u> be close to zero in general.

From (4.3.3), the determinantal equation for TM modes, when using the large argument approximation, is

$$\frac{J_o'(K_d a)}{J_o(K_d a)} = -j\frac{K_d}{K_m}\frac{\varepsilon_m}{\varepsilon_d} \qquad .....(4.5.1)$$

where K_m can be expressed in terms of λ_o, n, k as in Section 4.3

$$K_m a \cong \frac{2\pi a}{\lambda_o}(n-jk)$$

Under the condition that $\varepsilon_d=\varepsilon_o$, the determinantal equation can be expressed as:

$$\frac{J_o'(K_d a)}{J_o(K_d a)} = -j\frac{K_d a}{K_m a}\frac{\varepsilon_m}{\varepsilon_o} \cong -j\frac{K_d a}{K_m a}(n-jk)^2$$

$$= -jK_d a\frac{\lambda_o}{2\pi a}(n-jk)$$

Rearranging the above ,

$$\frac{J_o'(K_d a)}{(K_d a)J_o(K_d a)} = -j\frac{\lambda_o}{2\pi a}(n-jk) \qquad (4.5.2)$$

If $J_o(K_d a)$ could be zero, the right hand side of (4.5.2) would have to be infinite. However it will be shown here that the magnitude of the right hand side of (4.5.2) can be even smaller than 1.

For example, at λ_o=1.033μm, $n-jk$ = 0.272-j7.07 and for a/λ_o=20, the magnitude of the right hand side of (4.5.1) is about 1/20.

Now since the right hand side of (4.5.2) is small and $K_d a$ has approximately the value of its loss-free counterpart, which is not a large number (this will be confirmed by numerical methods in Chapter 5), $J_o(K_d a)$ can not be close to zero, otherwise it would lead to contradiction in (4.5.2). This implies that E_{zd} at the boundary can not be close to zero.

We conclude that such TM modes which can be deemed as the perturbed counterpart of TM modes in loss-free waveguides can not exist in microstructural guides at the wavelengths

of interest in this thesis. The TM modes which do exist will be configured very differently from those existing in lossfree guides

4.6 Characteristics of The Hybrid Modes

In the determinantal equation, if $m \neq 0$ both E_z and H_z exist. These are called hybrid modes.

It will be proved that for hybrid modes of reasonably small m, $J_m(K_d a) \longrightarrow 0$ and $J_m'(K_d a) \longrightarrow 0$ can <u>not</u> be true. This implies that neither $E\phi_d$ nor E_{zd} can be zero at the microstructural walls. We show this by assuming that $E\phi_d$ and E_{zd} are zero at the walls and then show that this assumption leads to a contradiction.

The simplified determinantal equation (4.3.1), when $\mu_d = \mu_m$, can be written as:

$$[J_m'(K_d a) + j\frac{K_d}{K_m} J_m(K_d a)][J_m'(K_d a) + j\frac{K_d \varepsilon_m}{K_m \varepsilon_d} J_m(K_d a)]$$

$$= -(\frac{\gamma m}{\omega a})^2 \frac{1}{\mu_d \varepsilon_d} (\frac{1}{K_d^2} - \frac{1}{K_m^2})^2 K_d^2 J_m^2(K_d a) \qquad .....(4.6.1)$$

Taking into consideration that $k^2 = \omega^2 \mu_d \varepsilon_d$, the right hand side of (4.6.1) becomes

$$- \frac{\gamma^2 m^2}{k^2} (1 - \frac{K_d^2}{K_m^2})^2 \frac{1}{(K_d a)^2} J_m^2(K_d a) \quad .....(4.6.1)^*$$

We will numerically verify in Chapter 5 that the value of $K_d a$ is approximately equal to its counterpart in a lossless waveguide. This means that for the mode of the lowest order, $K_d a$ will not have a value larger than 4. As we stated in Section 4.3, the smallest value of $K_m a$ is larger than 42. Hence we have,

$$\frac{K_d^2}{K_m^2} \ll 1$$

Thus by neglecting this term in (4.6.1)* and using $K_d^2=\gamma^2+k^2$, the right-hand side of (4.6.1) becomes:

$$-\frac{\gamma^2 m^2}{k^2}\frac{1}{(K_d a)^2}J_m^2(K_d a)=\frac{(k^2-K_d^2)m^2}{k^2}\frac{1}{(K_d a)^2}J_m^2(K_d a)$$

$$=m^2\left(1-\frac{K_d^2}{k^2}\right)\frac{1}{(K_d a)^2}J_m^2(K_d a)$$

So (4.6.1) is transformed into the following:

$$J_m'^2(K_d a)+j\frac{K_d\varepsilon_m}{K_m\varepsilon_d}J_m'(K_d a)J_m(K_d a)+j\frac{K_d}{K_m}J_m'(K_d a)J_m(K_d a)-\left(\frac{K_d}{K_m}\right)^2\frac{\varepsilon_m}{\varepsilon_d}J_m^2(K_d a)$$

$$=m^2\left(1-\frac{K_d^2}{k^2}\right)\frac{1}{(K_d a)^2}J_m^2(K_d a) \qquad .....(4.6.2)$$

In the left-hand side of (4.6.2), the third term is much smaller than the second term by a factor of $\varepsilon_m/\varepsilon_d$, (which we showed previously to be much larger than 1) and is, therefore, neglected

Thus (4.6.2) simplifies to:

$$J_m'^2(K_d a)+j\frac{K_d\varepsilon_m}{K_m\varepsilon_d}J_m'(K_d a)J_m(K_d a)-\left(\frac{K_d}{K_m}\right)^2\frac{\varepsilon_m}{\varepsilon_d}J_m^2(K_d a)$$

$$=m^2\left(1-\frac{K_d^2}{k^2}\right)\frac{1}{(K_d a)^2}J_m^2(K_d a) \qquad .....(4.6.3)$$

At this point, we suppose that:

$$J_m(K_d a)\longrightarrow 0$$

Neglecting the terms which have $J_m^2(K_d a)$, (4.6.3) becomes:

$$\frac{J_m'(K_d a)}{J_m(K_d a)}=-j\frac{K_d\varepsilon_m}{K_m\varepsilon_d}$$

This equation has the same form as the determinantal equation (4.5.1) for TM modes. Therefore by the same reasoning as that used in Section 4.5, we know that $J_m(K_d a)$ can <u>not</u> be close to zero.

As the next step we suppose that

$$J_m'(K_d a)\longrightarrow 0$$

Neglecting the term which has $[J_m'(K_d a)]^2$ in (4.6.3), we obtain:

$$\frac{J_m'(K_d a)}{J_m(K_d a)}=-j\frac{K_d}{K_m}-jm^2\frac{K_m\varepsilon_d}{K_d\varepsilon_m}\left[1-\left(\frac{K_d}{k}\right)^2\right]\frac{1}{(K_d a)^2}$$

Thus we obtain

$$\frac{J_m'(K_d a)}{J_m(K_d a)}=-j\frac{K_d}{K_m}-jm^2\frac{K_m\varepsilon_d}{K_d\varepsilon_m}\frac{1}{(K_d a)^2}+jm^2\frac{K_m\varepsilon_d}{K_d\varepsilon_m}\frac{1}{(ka)^2}$$

$$.....(4.6.4)$$

Applying $K_m a \cong \frac{2\pi a}{\lambda_o}(n-jk)$ and $\varepsilon_d/\varepsilon_m = \varepsilon_o/\varepsilon_m = 1/(n-jk)^2$ the three terms on the right-hand side of (4.6.4) can be written as:

first term : $-j(K_d a)\frac{\lambda_o}{2\pi a}\frac{1}{(n-jk)}$

second term : $-j\frac{m^2}{(K_d a)^3}\frac{2\pi a}{\lambda_o}\frac{1}{(n-jk)}$

third term : $+j\frac{m^2}{(K_d a)}\frac{\lambda_o}{2\pi a}\frac{1}{(n-jk)}$

If $J_m'(K_d a)$ could be close to 0, then the right hand side of (4.6.4) would have to be close to zero. However we will show here that the right hand side of (4.6.4) can be a number much larger than zero.

Estimating the values of the above three terms in a similar fashion as in Section 4.4 and 4.5, we can see that the first and the third terms are close to zero. But if a/λ_o is 20, and say λ_o=1.033μm, where $n-jk$=0.272+j7.07, then the second term is roughly about 1. Therefore, the right-hand side of (4.6.4) is not very small and $J_m'(K_d a)$ can <u>not</u> be close enough to zero that perturbation methods can be applied.

Thus a hybrid mode will have significant tangential fields E_z and $E\phi$ at the waveguide walls.

Since for hybrid modes both E_z and H_z exist we will next define a quantity which by its magnitude measures the dominance of the longitudinal electric field E_z over the longitudinal magnetic field H_z.

Equation (4.2.3) gives the ratio of the amplitudes of

both these field components at their respective maxima in their dependence on ϕ. The ratio has the dimension of an impedance. In a homogeneous medium, a plane wave has the wave impedance (intrinsic impedance)[23]

$$\eta_c = j\frac{\omega\mu_o}{\gamma}$$

where μ_o is the permittivity of free space.

Let us now define a factor,

$$R = \eta_c \frac{B_m}{A_m}$$

Taking into consideration that

$$E_{zd}=A_m J_m(K_d r)\cos(m\phi)\ e^{-\gamma z}$$

$$H_{zd}=B_m J_m(K_d r)\sin(m\phi)\ e^{-\gamma z}$$

R tells us to what extent the ratio $\frac{A_m}{B_m}$ differs from the plane wave impedance in a medium. For $|R|<1$, E_z dominates over H_z compared to the ratio of E_z to H_z in a uniform plane wave. It is an E-like mode.

$|R|>1$ means that the magnetic field dominates over the electric field. It is an H-like mode.

From (4.2.4) we have,

$$\frac{B_m}{A_m} = \frac{\left(\frac{\varepsilon_d}{K_d}\frac{J_m'(K_d a)}{J_m(K_d a)} - \frac{\varepsilon_m}{K_m}\frac{H_m^{(2)\prime}(K_m a)}{H_m^{(2)}(K_m a)}\right)^{1/2}}{\left(\frac{\mu_d}{K_d}\frac{J_m'(K_d a)}{J_m(K_d a)} - \frac{\mu_m}{K_m}\frac{H_m^{(2)\prime}(K_m a)}{H_m^{(2)}(K_m a)}\right)^{1/2}}$$

Therefore R can be written as

$$R = j\frac{\omega\mu}{\gamma} \frac{\left(\frac{\varepsilon_d}{K_d}\frac{J_m'(K_d a)}{J_m(K_d a)} - \frac{\varepsilon_m}{K_m}\frac{H_m^{(2)\prime}(K_m a)}{H_m^{(2)}(K_m a)}\right)^{1/2}}{\left(\frac{\mu_d}{K_d}\frac{J_m'(K_d a)}{J_m(K_d a)} - \frac{\mu_m}{K_m}\frac{H_m^{(2)\prime}(K_m a)}{H_m^{(2)}(K_m a)}\right)^{1/2}}$$

It is readily seen from (4.2.1) and (4.2.2) that for TE modes $R=\infty$, and for TM modes $R=0$.

R will be used in Chapter 5 as a criterion to decide what kind of mode a specific numerical value of γ represents.

5 NUMERICAL RESULTS FOR CYLINDRICAL MICROSTRUCTURAL WAVEGUIDES

5.1 Numerical Methodology

In Chapter 4 we discovered that for TM and hybrid modes, because the real physical system differs significantly from the ideal microwave model, the perturbation method can not be applied. Consequently, in a microstructural guide, the TM and hybrid modes will be configured very differently from their counterparts in a microwave waveguide. The field configurations of TM and hybrid modes are not readily known. Thus it makes the field analysis prohibitively difficult. As a preliminary attempt to solve this difficult problem, however, we will use a numerical method to calculate the propagation constants of the TM_{01} mode and one hybrid mode.

For our numerical work of solving the determinantal equation for the root γ, weuse a software package named Mulrun-General. Its numerical analysis is based on Muller's method, which is an algorithm for finding the complex roots of equations. We now explain it in some detail.

If all the terms of the determinantal equation are taken to one side, then the equation of which the solution is to be found is of the form

$$f(x) = f_1(x) - f_2(x) = 0 \qquad .....(5.1.1)$$

Suppose we know the values of f(x) for three distinct values a, b, c. They are f(a), f(b), f(c). We call a,b and c initial values.

We can construct a second degree polynomial P(x) such that

$$P(a)=f(a),\ P(b)=f(b),\ P(c)=f(c)$$

We find the zeros of P(x) and select one of them, d, to be a new initial value which is better than the former ones a,b, and c in the sense that it is closer to the solution. We repeat the process again by using b, c and d as a new set of initial values to find a better new initial value and so on. An illustration of this process is shown in Fig.4.

The advantage of Muller's method is that it can be carried out using only the values of the function f(x) itself. As for our software package Mulrun-General, we will need only one approximate value of γ, which we call the initial estimate. The other two values will be chosen automatically by the program.

Muller's method has two disadvantages and they are:
(1) This algorithm will give several solutions for one equation. We have to decide which one is the right one. For every zero q, the algorithm will evaluate (5.1.1) at q, namely, $f(q)=f_1(q)-f_2(q)$.

Because q is the zero of f(q), theoretically f(q) should be zero. However for a computer algorithm, f(q)

generally is not exactly equal to zero even though it is a very small number.

The problem is how to decide if f(q) is small enough so that we can accept q as the numerical root.

Here we choose the zero q so that f(q) is smaller than $f_1(q)$ or $f_2(q)$ by at least a factor of the order of 10^{-10}. We may obtain more than one q satisfying this criterion. In this case we choose the q which yields the smallest value of f(q) and at the same time is physically meaningful.

(2) The numerical roots obtained depend on the initial values, especially if the equation has several roots. If we select the initial values far from the desired root, the root obtained may not be the correct one. Thus the precondition for obtaining a correct numerical root is that we have initial values close to the desired root.

This may cause a serious problem in trying to solve a determinantal equation, because it will have many roots with each one representing a different mode. Thus if for a specific mode we choose initial estimates which are too far from the correct value of the root, we can end up with a root from another mode.

It should be pointed out here that even though the propagation constant γ of TM or hybrid modes is not the perturbed one of its microwave counterpart, the γ obtained from the latter (microwave counterpart) is still useful as an initial value. This is due to the fact that the imaginary

part of γ is approximately the same for both the actual lossy physical system and the microwave counterpart as mentioned in Section 4.3. We derive an expression for γ in the Appendix.

In Section 5.2, the Hankel function approximation used in our analytical analysis in Chapter 4 is numerically justified.

In Section 5.3, we compute the numerical solutions of the determinantal equation for the TE_{01} mode, using the analytical results as initial values.

In Section 5.4, we use the results from the Appendix as the initial values to obtain numerical attenuation constants for the TM_{01} mode for a/λ_o from 1 to 20. As mentioned above, the formula for the propagation constants of the TM_{01} mode from the Appendix does not represent the true physical propagation constants in general, which means the initial values for Muller's algorithm may not be very close to the true physical values of the TM_{01} mode. Thus we have to confirm that the attenuation constant for every value of a/λ_o is indeed from the TM_{01} mode. We do this by examining the radial variation of E_{zd}, to determine which zero of the Bessel function $J_o(K_d r)$ or $J_1(K_d r)$ lies near the waveguide wall.

In Section 5.5, we analyze a hybrid mode of lowest order, which means it is the counterpart of the TE_{11} mode of a microwave waveguide. In other words, we begin by

propagating a TE_{11} mode in a loss-free microwave waveguide, and then gradually change the guide wall to a material which assumes the refractive index of a gold film for infrared radiation, as listed in TABLE I. We call this wave the lowest order hybrid mode. The numerical attenuation constants are obtained for this mode for a/λ_o from 1 to 20 using values from the formula for the TE_{11} mode in the Appendix as the initial values. We show that these attenuation constants for a/λ_o in a range 1 to 20 do not specifically represent an E-like wave or an H-like wave. This means that for some values of a/λ_o the attenuation constants represent an E-like wave but for other values they represent an H-like wave.

We are obliged to remind the reader that the numerical analysis here is preliminary in the perspective of future work. We are tackling here a problem as large, complicated and original as the development of optical fibers. We are developing hollow micrometer-sized metal-coated optical waveguide theory!

One of the important achievements in this research is that we prove that for waveguides of circular-cross section, the microwave waveguide is not universally applicable as an model for a microstructural guide. For the latter, the propagation characteristics are in general <u>not</u> perturbed cases of the former, although it is true for TE modes. Thus the field distributions of the other modes can not be

obtained by perturbing their microwave counterparts.

Unfortunately, a full understanding of the propagation characteristics for TM and hybrid modes of microstructural cylindrical waveguides depends on the knowledge of field distributions of these modes. The field distributions appear to be so complex that a detailed study is simply beyond the scope of this investigation.

5.2 Asymptotic Behavior of Hankel Functions

In Section 4.3, we mentioned that :

$$\frac{H_m^{(2)\prime}(K_m a)}{H_m^{(2)}(K_m a)} \longrightarrow -j$$

In this work the magnitude of $K_m a$ is always larger than or equal to about 40. We can not, *a priori*, decide if this value is large enough so that the above approximation is adequate to permit accurate determination of the propagation constant γ from the determinantal equation (3.2.18).

For the purpose of obtaining more precise numerical results, and verifying that the simplified form of the determinantal equation is accurate enough for theoretical analysis, we have to use the asymptotic series expression for Hankel functions. From [27], [28] :

$$H_m^{(2)}(x) = \left(\frac{2}{\pi x}\right)^{1/2} e^{-j[x-m\pi/2-\pi/4]} \sum_{s=0}^{Q} \frac{1}{(2jx)^s} \frac{\Gamma(m+s+\frac{1}{2})}{\Gamma(s+1)\Gamma(m-s+\frac{1}{2})} + O(x^{-Q})$$

Similarly, we have

$$H_{m+1}^{(2)}(x) = \left(\frac{2}{\pi x}\right)^{1/2} e^{-j[x-m\pi/2-3\pi/4]} \sum_{s=o}^{Q} \frac{1}{(2jx)^s} \frac{\Gamma(m+s+\frac{3}{2})}{\Gamma(s+2)\Gamma(m-s+\frac{3}{2})} + O(x^{-Q})$$

Here O is the Bachman-Landau symbol which denotes a function of the order of magnitude of x^{-Q}.

In Section 4.3, we mentioned that

$$\frac{H_m^{(2)\prime}(x)}{H_m^{(2)}(x)} \equiv \frac{m}{x} - \frac{H_{m+1}^{(2)}(x)}{H_m^{(2)}(x)}$$

We can calculate a more accurate value of $\frac{H_m^{(2)\prime}(x)}{H_m^{(2)}(x)}$ than that of section 4.3, numerically.

For $x=K_m a$ of interest in this research, if $Q=50$, the term $(K_m a)^{-Q} \cong 42^{-50}$ which is small compared to the explicit summation of the asymptotic series for the Hankel functions. By numerical calculation, we find that the approximation

$$\frac{H_m^{(2)\prime}(K_m a)}{H_m^{(2)}(K_m a)} = -j$$

is generally accurate to within 0.5% . This value justifies the use of the approximation in our analytical analysis in Chapter 4.

For more precise numerical solutions of the determinantal equation, we use in our numerical calculations the series representation of the Hankel function given above.

5.3 Numerical Results for TE_{01} Mode

As we stated in Section 4.4, the perturbation method and power flow method can be applied to TE modes. Using both methods, we have obtained analytical formulas for the attenuation constant. The formulas obtained by the two different approaches agree with each other. We are going to further verify this agreement using numerical calculations. The numerical analysis method will be explain here in some detail.

The determinantal equation for TE modes can be expressed as (4.2.1)

$$\frac{\mu_d J_o'(K_d a)}{K_d J_o(K_d a)} - \frac{\mu_m H_o^{(2)}'(K_m a)}{K_m H_o^{(2)}(K_m a)} = 0 \quad .....(4.2.1)$$

In this equation, μ_d and μ_m are known constants of the materials. The unknown variables are K_d and K_m. which are related to γ by,

$$K_d^2=\gamma^2+\omega^2\mu_d\varepsilon_d \ , \qquad K_m^2=\gamma^2+\omega^2\mu_m\varepsilon_m$$

Hence the only unknown is the parameter γ; i.e. γ is the root of (4.2.1). The values of γ obtained in Section 4.4 by analytical methods will be used here as initial estimate

for Muller's algorithm.

More specifically, we use pairs of α and β as initial estimates. α is derived in Section 4.4. We rewrite it here as

$$\alpha_{TEon} = \frac{1}{a}\frac{n}{n^2+k^2}\left(\left(\frac{p_{1n}\lambda_o}{2\pi a}\right)^2 \Big/ \sqrt{1-\left(\frac{p_{1n}\lambda_o}{2\pi a}\right)^2} \right) \qquad .....(4.4.4)$$

We will calculate β from the expression for γ derived in section 4.4, namely

$$\gamma = jk\left(\left(1-\left(\frac{p_{1n}\lambda_o}{2\pi a}\right)^2\right)^{1/2} - \frac{1}{2}\left(1-\left(\frac{p_{1n}\lambda_o}{2\pi a}\right)^2\right)^{-1/2}\left(\left(\frac{p_{1n}\lambda_o}{2\pi a}\right)^2 2j\frac{\lambda_o}{2\pi a}\frac{1}{(n-jk)}\right)\right)$$

since $\beta = Im(\gamma)$, we obtain,

$$\beta = k\left(1-\left(\frac{p_{1n}\lambda_o}{2\pi a}\right)^2\right)^{1/2} + k\left(1-\left(\frac{p_{1n}\lambda_o}{2\pi a}\right)^2\right)^{-1/2}\left(\frac{p_{1n}\lambda_o}{2\pi a}\right)^2 \frac{\lambda_o}{2\pi a}\frac{k}{n^2+k^2}$$

Keeping in mind $k = \frac{2\pi}{\lambda_o}$, we have,

$$\beta = \frac{2\pi}{\lambda_o}\left(1-\left(\frac{p_{1n}\lambda_o}{2\pi a}\right)^2\right)^{1/2} + \left(1-\left(\frac{p_{1n}\lambda_o}{2\pi a}\right)^2\right)^{-1/2}\left(\frac{p_{1n}\lambda_o}{2\pi a}\right)^2 \frac{1}{a}\frac{k}{n^2+k^2}$$

Then we calculate the pairs of α and β as initial estimates of γ for a/λ_o in the range 0.5-20.

By using those initial estimates we finally obtain the numerical solutions of the determinantal equation. The

results are virtually the same as theoretical ones for $a/\lambda_o>1$. Therefore our analytical formulas for TE modes would seem to be accurate for all practical purposes.

The attenuation constants of the TE_{01} mode obtained by both numerical and analytical methods for $\lambda_o=1.033\mu m$ and $\lambda_o=9.919\mu m$ are given in TABLE II and TABLE III respectively.

The deviation of analytical results from numerical results is less than 12% for the worst case.

Another important concept for waveguides is propagation distance, which is defined as the number of free space wavelengths that the wave will propagate before its intensity is reduced to 1/e of its initial value. The propagation distance is given by $1/\alpha\lambda_o$.

We show the propagation distances of the TE mode at $1.033\mu m$ and $9.919\mu m$ respectively in Fig.5 and Fig.6.

From Fig.5 and Fig.6, it is evident that the propagation distances are of the order of several centimeters for TE_{01} modes.

The deviation of the approximate analytical results from accurate numerical results is just as it is expected to be. That is, as a/λ_o becomes smaller, the deviation becomes larger. The reason for this can be seen by considering the following:

From the determinantal equation (4.4.1)

$$\frac{J_o'(K_d a)}{(K_d a)J_o(K_d a)} = -j\frac{\lambda_o}{2\pi a}\frac{1}{(n-jk)} \qquad .....(4.4.1)$$

we see that as a/λ_o becomes smaller, the right hand side of the equation becomes larger. Therefore for some sufficiently small values of a/λ_o the precondition for perturbation, which requires a small departure of the physical system from the loss-free model, is no longer satisfied. Therefore the theoretical results obtained by the perturbation method become invalid for very small a/λ_o.

As we will see later the TE_{01} mode is the most loss-free mode in a microstructural cylindrical waveguide, while the most loss-free mode for a microstructural parallel-plate waveguide is the TE_{10} mode[22].

Comparing the expression of the attenuation constant for the TE_{01} mode of cylindrical microstructural waveguides with that for TE_{10} mode of parallel-plate microstructural waveguides[22] by taking radius of cylindrical guide and plate-spacing of parallel-plate guide as comparable counterparts, we see the cylindrical one is roughly 1/2 of the parallel-plate one.

5.4 Numerical Results for TM_{01} Mode

We have pointed out already in Section 4.5 that the perturbation and power flow methods can not be used to derive the propagation constants for TM modes. Because the actual physical system differs significantly from the ideal

model we are not able to obtain an analytical solution of the determinantal equation in this case.

According to the analysis of Sections 4.4 and 4.5, TE modes do not differ very much from the ideal lossless TE modes, but TM modes deviate greatly from the ideal lossless TM modes. It implies that for cylindrical microstructural waveguides TM modes are much more heavily attenuated than TE modes. This means that the differences in the attenuation constants of TE modes and TM modes of micron-sized waveguides are much larger than for microwave waveguides.

Because we can not obtain a formula for γ for TM modes of microstructural waveguides by analytical methods, we are going to use the formulas obtained in the Appendix as initial estimates for Muller's method. For convenience, we present the determinantal equation (4.2.2) for TM modes here:

$$\frac{\varepsilon_d J_o'(K_d a)}{K_d J_o(K_d a)} - \frac{\varepsilon_m H_o^{(2)\prime}(K_m a)}{K_m H_o^{(2)}(K_m a)} = 0$$

The initial estimate for γ from (A.2.1) in the Appendix is

$$\gamma = jk\left[\left(1 - \left(\frac{p_{on}\lambda_o}{2\pi a}\right)^2\right)^{1/2} - \frac{1}{2}\left(1 - \left(\frac{p_{on}\lambda_o}{2\pi a}\right)^2\right)^{-1/2}\frac{\lambda_o}{j\pi a}\,\frac{1}{n-jk}\right]$$

Since $\alpha = \mathrm{Re}(\gamma)$, $\beta = \mathrm{Im}(\gamma)$, we can write

$$\alpha = \frac{1}{a}\frac{n}{n^2+k^2}\left(1/\sqrt{1-\left(\frac{p_{on}\lambda_o}{2\pi a}\right)^2}\right)$$

$$\beta = \frac{2\pi}{\lambda_o}\left(1-\left(\frac{p_{on}\lambda_o}{2\pi a}\right)^2\right)^{1/2} + \left(1-\left(\frac{p_{on}\lambda_o}{2\pi a}\right)^2\right)^{-1/2}\frac{1}{a}\frac{k}{n^2+k^2}$$

We use the same numerical analysis method as in Section 5.2. The attenuation constants for λ_o=1.033μm and 9.919μm can be obtained, as shown in Fig.7 and Fig.9. The propagation distances for λ_o=1.033μm and λ_o=9.919μm are shown in Fig 8 and Fig.10 respectively. They are in the range of several millimeters.

When we are using the numerical method, we actually calculate γ for different discrete values of a/λ_o (0.7, 1, 2, 3,$\cdots$ 20).

This means we have 21 sample points. It is possible that for a value of a/λ_o, the numerical root γ may not represent the TM_{01} mode (the meaning of TM_{on} modes for microstructural waveguides is explained later in this section) due to the fact that the initial estimates α and β are only valid for $\sqrt{\varepsilon_m/\varepsilon_d} \gg a/\lambda_o$ which no longer holds for microstructural waveguides. γ obtained numerically from (4.2.2) using the initial estimates which are not very close to the actual roots of TM_{01} may be the roots of TM_{02}, TM_{03}... etc.

Fortunately our numerical values do correspond to the roots of the TM_{01} mode as a/λ_o varies from 1 to 20. We can

see this by analogy with the ideal perfect conductor case.

For a lossless waveguide, we can plot the radial variation of E_{zd} by fixing ϕ to an arbitrary value. This plot is shown in Fig.11. E_{zd} varies as $J_o(K_d r)$ in its radial variation. Fig.11 represents a normalized plot of E_{zd}, as given by (3.2.1)* .

For ideal lossfree waveguides, if $K_d a = p_{01}$ we call it a TM_{01} mode; if $K_d a = p_{02}$ we call it a TM_{02} mode and so on.

In microstructural waveguides, because the TM_{01} modes are heavily perturbed compared with those of lossfree waveguides, we can not expect $K_d a = p_{01}$. But if for a particular a/λ_o the radial value of E_{zd} does not go through the first zero of $J_o(K_d r)$ in the interior of the guide, we designate the mode as the TM_{01} mode.

The radial variation of E_{zd} for the TM_{01} mode at the free space wavelength 1.033μm for both a/λ_o=1 and 20 are depicted in Fig.12 and Fig.13, respectively. The values of K_d used to plot these figures is obtained from the numerically obtained values of γ and $K_d^2 = \gamma^2 + \omega^2 \mu_d \varepsilon_d$.

Similarly in Fig.14 and Fig.15, we show the radial variation of E_{zd} at 9.919μm for a/λ_o=1 and 20, respectively.

Comparing Figs.12-15 with Fig.11, we can see that the radial values of E_{zd} for λ_o and a/λ_o of interest in this work <u>do not</u> go through the <u>first zero</u> of $J_o(K_d r)$ in the interior of the guide.

Therefore we conclude that attenuation constants

obtained by the numerical method for different a/λ_o are indeed of the same mode, i.e. the TM_{01} mode.

It should be reiterated here that the electric field intensity of the TM_{01} mode at the guide walls of microstructural cylindrical waveguides is significant and therefore the losses are quite large.

5.5 Numerical Results for a Hybrid Mode

From (3.2.18), the determinantal equation for hybrid modes can be written as,

$$\left(\frac{\mu_d}{K_d}\frac{J_m'(K_d a)}{J_m(K_d a)} - \frac{\mu_m}{K_m}\frac{H_m^{(2)}{}'(K_m a)}{H_m^{(2)}(K_m a)}\right)\times \left(\frac{\varepsilon_d}{K_d}\frac{J_m'(K_d a)}{J_m(K_d a)} - \frac{\varepsilon_m}{K_m}\frac{H_m^{(2)}{}'(K_m a)}{H_m^{(2)}(K_m a)}\right) + \left(\frac{\gamma m}{\omega a}\right)^2\left(\frac{1}{K_d^2} - \frac{1}{K_m^2}\right)^2 = 0$$

We use formula (A.1.2) in the appendix for m=1 to calculate the values of initial estimates, because we hope to find the hybrid mode which is degenerate from TE_{11}. For m=1 n=1, (A.1.2) becomes

$$\gamma = -jk\left[1-\left(\frac{p'_{11}\lambda_o}{2\pi a}\right)^2 + 2j\left(\frac{p'_{11}\lambda_o}{2\pi a}\right)^2 (1/ak)\frac{1}{n-jk} + 2j\frac{1}{p'^2_{11}-1}(1/ak)\frac{1}{n-jk}\right]^{1/2}$$

We have

$$\alpha = \frac{1}{a}\frac{n}{n^2+k^2}\left(\left(\frac{p_{i1}\lambda_o}{2\pi a}\right)^2 + \frac{1}{p_{i1}^2-1}\right)\Big/\left(1-\left(\frac{p_{i1}\lambda_o}{2\pi a}\right)^2\right)^{1/2}$$

$$\beta=\frac{2\pi}{\lambda_o}\left[1-\left(\frac{p_{i1}\lambda_o}{2\pi a}\right)^2\right]^{1/2}+\left[1-\left(\frac{p_{i1}\lambda_o}{2\pi a}\right)^2\right]^{-1/2}\left(\left(\frac{p_{i1}\lambda_o}{2\pi a}\right)^2+\frac{1}{p_{i1}^2-1}\right)\frac{1}{a}\frac{k}{n^2+k^2}$$

Therefore by applying Muller's method, we can obtain the numerical solution of the determinantal equation, namely, the attenuation constants, which are shown in Fig.16 and Fig.18 for 1.033μm and 9.919μm respectively. The corresponding propagation distances are plotted in Fig.17 and Fig.19.

As a next step, we will check if the numerical results for different a/λ_o are of an H-like wave.

Similar to Section 5.4, as a reference we plot $J_1'(K_d r)$ for an ideal lossless waveguide in Fig.20.

In order to see if the curve of the magnitude of $J_1'(K_d r)$ of our microstructural waveguides goes through its first zero, we plot the magnitude of $J_1'(K_d r)$ versus the magnitude of $K_d r$, as shown in Figs.21 and 22 for 1.033μm and Figs.23 and 24 for 9.919μm. For K_d we use again a value obtained from the numerically calculated value of γ and $K_d^2=\gamma^2+\omega^2\mu_d\varepsilon_d$.

Comparing Fig.21 with Fig.22, we see that the curvature for the magnitude of $J_1'(K_d r)$ at $a/\lambda_o=2$(Fig.21) is very different from its counterpart at $a/\lambda_o=3$(Fig.22). The same phenomenon can be observed for $a/\lambda_o=18$, 19 when we

compare Fig.23 with Fig.24.

We now give the explanation for this surprising phenomenon:

We defined R in Chapter 4 as,

$$R = j\frac{\omega\mu}{\gamma}\ \frac{\left(\frac{\varepsilon_d}{K_d}\ \frac{J_m'(K_d a)}{J_m(K_d a)} - \frac{\varepsilon_m}{K_m}\ \frac{H_m^{(2)\prime}(K_m a)}{H_m^{(2)}(K_m a)}\right)^{1/2}}{\left(\frac{\mu_d}{K_d}\ \frac{J_m'(K_d a)}{J_m(K_d a)} - \frac{\mu_m}{K_m}\ \frac{H_m^{(2)\prime}(K_m a)}{H_m^{(2)}(K_m a)}\right)^{1/2}}$$

In the expression for R, constants of the materials μ_d, μ_m, ε_d and ε_m are known; K_d, K_m can be obtained from γ. Hence if we know γ, R can be determined.

Therefore we can calculate $|R|$ for different a/λ_o from 1 to 20 for 1.033μm and 9.919μm respectively, as shown in Fig.25 and Fig.26.

If we study Figs.20-22 carefully, we observe that for 1.033μm:

If $a/\lambda_o=2$, where $|R|<1$, the curve of the magnitude of $J_1'(K_d r)$ (Fig.21) is of a form similar to that of Fig.20.

If $a/\lambda_o=3$, where $|R|>1$, the curve of the magnitude of $J_1'(K_d r)$ (Fig.22) is of a form completely different to that of Fig.20.

Similarly, from Figs.20, 23, and 24, we observe the same phenomenon for 9.919μm.

This is not a mere coincidence. When the magnitude of R is larger than 1 the axial magnetic field intensity is

weighted more than the axial electric field intensity. To put it another way we have an H-like mode. When the magnitude of R is smaller than 1 the axial electric field intensity dominates over the magnetic field intensity, and we have an E-like mode. Therefore the nature of the mode changes here.

If we observe $K_d r$ as the change from an H-like mode to an E-like mode occurs, we discover the real part of $K_d r$ changes from being larger than the imaginary part to it being smaller than the imaginary part.

6 CONCLUSIONS

An investigation has been done to evaluate the propagation losses for infrared radiation in empty, gold-coated microstructural waveguides of circular cross section as a first step in understanding propagation in a closed hollow microstructural waveguide.

In spite of the complexity of propagation characteristics of microstructural cylindrical waveguides, we have been able to identify several important features about wave propagation. These are:

(I) Three kinds of modes exist. They are TE modes, TM modes and Hybrid modes.

(II) By analyzing the determinantal equation, we have shown that for TE modes the tangential components of the electric fields at the guide walls, much like the electric fields in a microwave waveguide at microwave frequencies, are very small. Thus we expect low losses for TE modes. This result is also verified numerically.

(III) The formulas for attenuation constants of TE modes are obtained by analytical methods. The formulas are checked against the results obtained by the power flow method and by numerical methods. Furthermore, the formula agrees with that for the attenuation constant in a microwave guide in the limit as the conductivity of the waveguide walls is assumed to be very large.

(IV) Propagation distances to 1/e attenuation of many centimeters are theoretically possible for TE modes, when the ratio of waveguide radius to free space wavelength is larger than 1.

(V) By analyzing the determinantal equation we have found that for TM modes or hybrid modes the tangential electric fields at the guide walls usually can not be close to zero. This means that the propagation losses are relatively large. This result is verified by numerically-calculated attenuation constants for these modes.

In this respect, wave propagation in a microstructural circular waveguide differs markedly from wave propagation in a normal microwave waveguide, in which propagation losses are relatively low. This is believed to be a new result which has not previously been reported.

(VI) For TM and hybrid modes, the propagation distances are of the order of several millimeters, when $a/\lambda_o \geq 1$.

(VII) For the hybrid mode, the mode undergoes changes at some specific a/λ_o, where it changes from an H-like mode to an E-like mode. This is an inherent feature of cylindrical microstructural waveguides.

(VIII) The attenuation constants for cylindrical microstructural waveguides are approximately one half those of the parallel plate counterparts[22] for the same value of plate-spacing and guide radius.

Our results for microstructural waveguides of circular cross-section provide valuable physical insight into wave propagation at infrared wavelengths in micrometer-sized waveguides. The results obtained are also of practical value in potential application of closed microstructural guides.

It is suggested that future investigations examine wave propagation in closed microstructural guides of those non-circular cross-sections that can readily be fabricated, such as those of triangular, rectangular and trapezoidal cross-sections and that the theoretical results obtained be compared to experimentally obtained results.

TABLE I [25]

The Complex Refractive Index for Evaporated Gold Film

$\lambda_o(\mu m)$	n	k	$\varepsilon'/\varepsilon_o$	$\varepsilon''/\varepsilon_o$
9.919	12.24	54.7	-2842	1339
4.959	3.748	30.5	-916.2	228.6
2.000	0.850	12.6	-158.0	21.42
1.033	0.272	7.07	-49.91	3.846

TABLE II

Attenuation Constant (1/meter) of TE_{01} Mode at 1.033μm

a/λ_o	ANALYTICAL	NUMERICAL
0.7	11625	9208
1	2469	2175
2	257	238
3	74	70
4	31	30
5	15.8	15.5
15	0.6	0.6
20	0.2	0.2

TABLE III

Attenuation Constant (1/meter) of TE_{01} Mode at 9.919μm

a/λ_o	ANALYTICAL	NUMERICAL
0.7	848	843
1	184	182
2	19.17	19.15
3	5.52	5.51
4	2.31	2.31
5	1.17	1.17
15	0.04	0.04
20	0.018	0.018

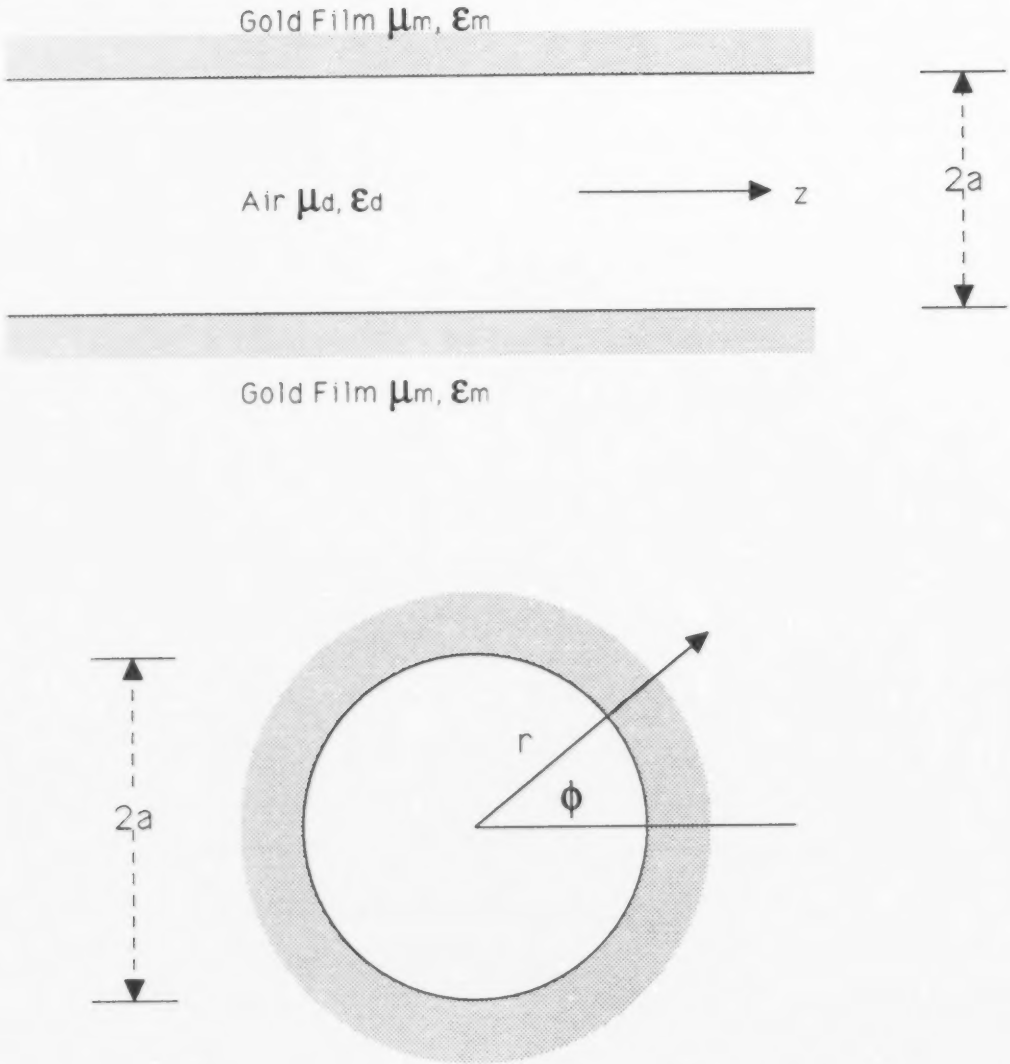

Fig.1 Geometry of Cylindrical Microstructural Waveguide

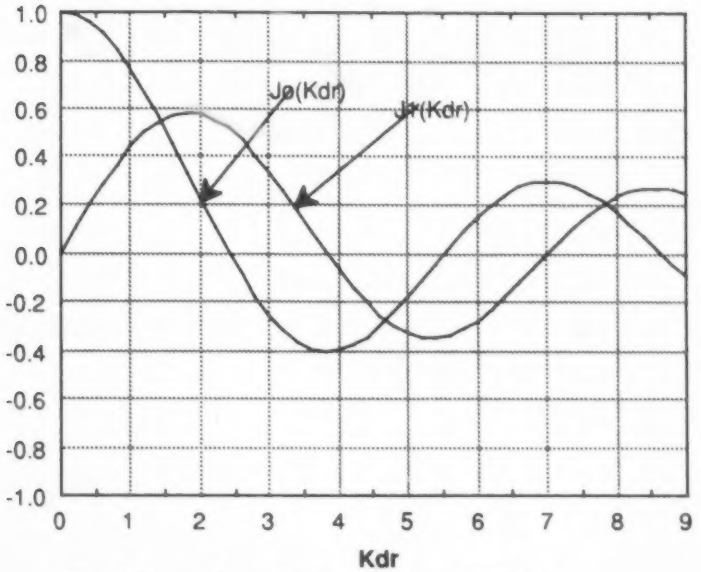

Fig. 2 Bessel Functions $J_o(Kar)$ and $J_1(Kar)$

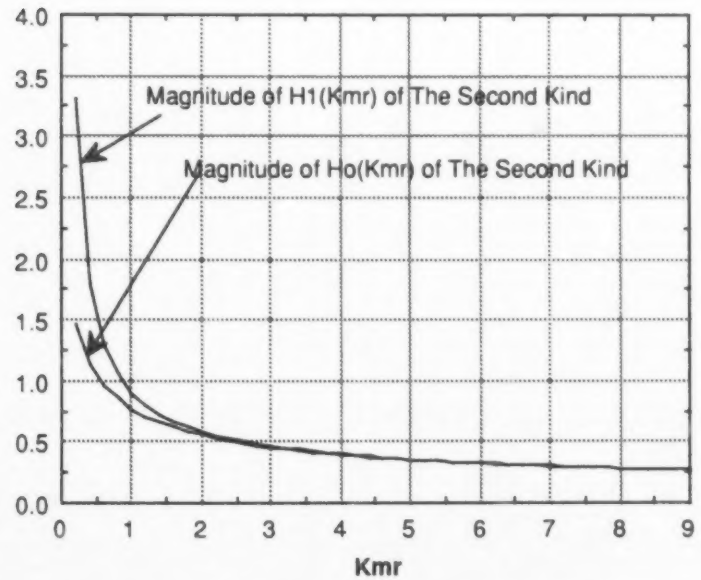

Fig. 3 Hankel Functions $|H_o^{(2)}(kmr)|$ and $|H_1^{(2)}(Kmr)|$

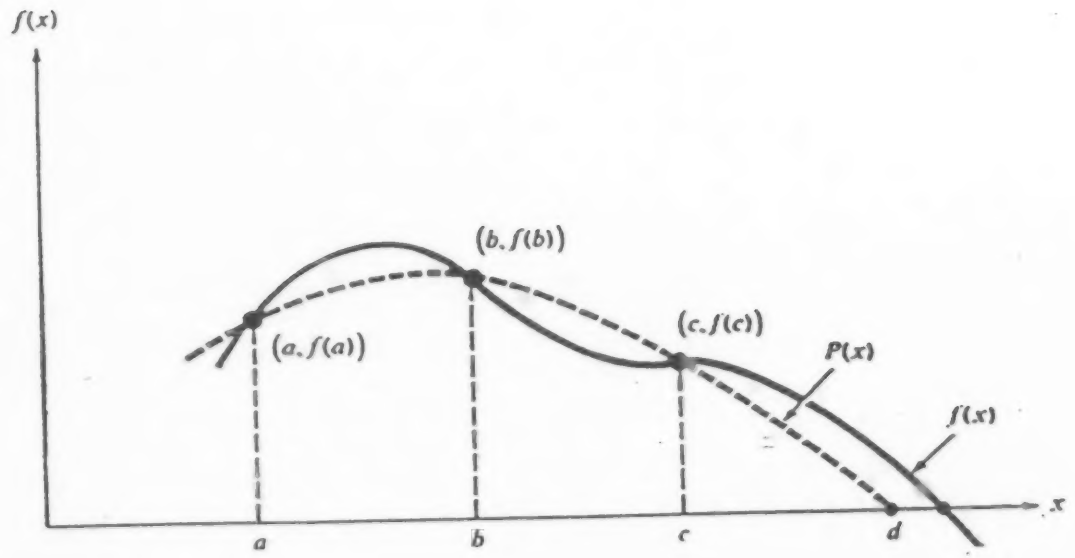

Fig.4 Illustration of Muller's Method

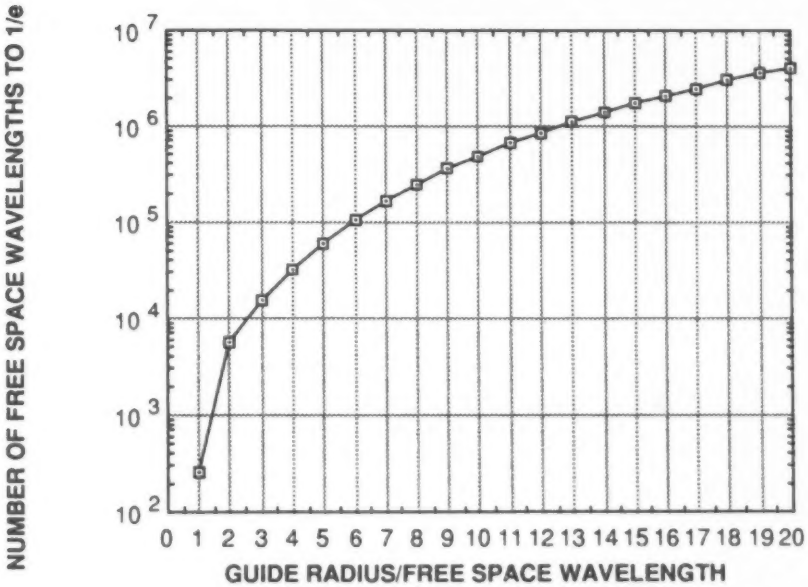
NUMBER OF FREE SPACE WAVELENGTHS TO 1/e
10 7
10 6
10 5
10 4
10 3
10 2
0 1 2 3 4 5 6 7 8 9 10 11 12 13 14 15 16 17 18 19 20
GUIDE RADIUS/FREE SPACE WAVELENGTH

Fig.5 Propagation Distance of the TE_{01} Mode at 1.033 μm

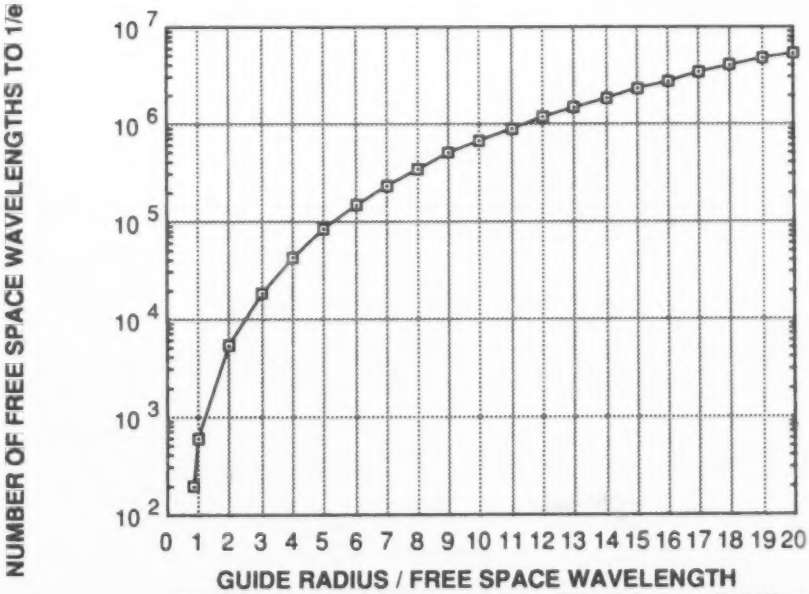
NUMBER OF FREE SPACE WAVELENGTHS TO 1/e
10 7
10 6
10 5
10 4
10 3
10 2
0 1 2 3 4 5 6 7 8 9 10 11 12 13 14 15 16 17 18 19 20
GUIDE RADIUS / FREE SPACE WAVELENGTH

Fig.6 Propagation Distance of the TE_{01} Mode at 9.919 μm

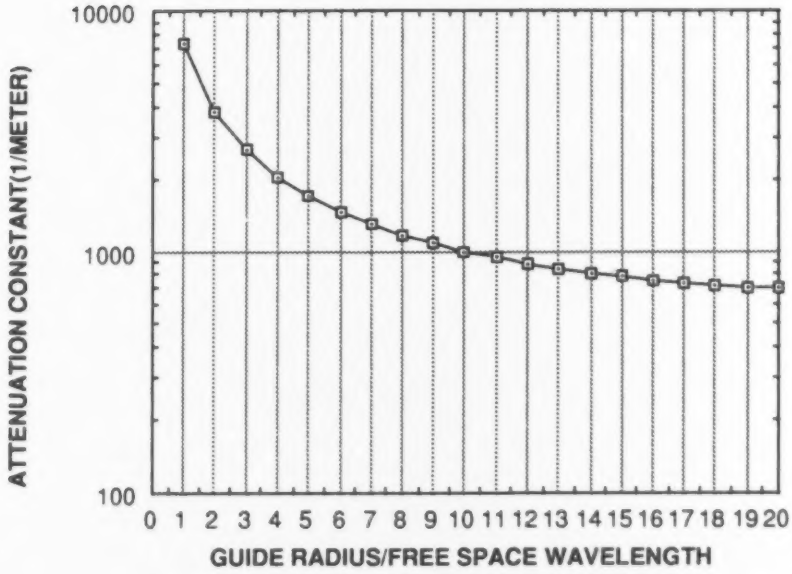

Fig.7 Attenuation Constant of the TM_{01} Mode at 1.033 μm

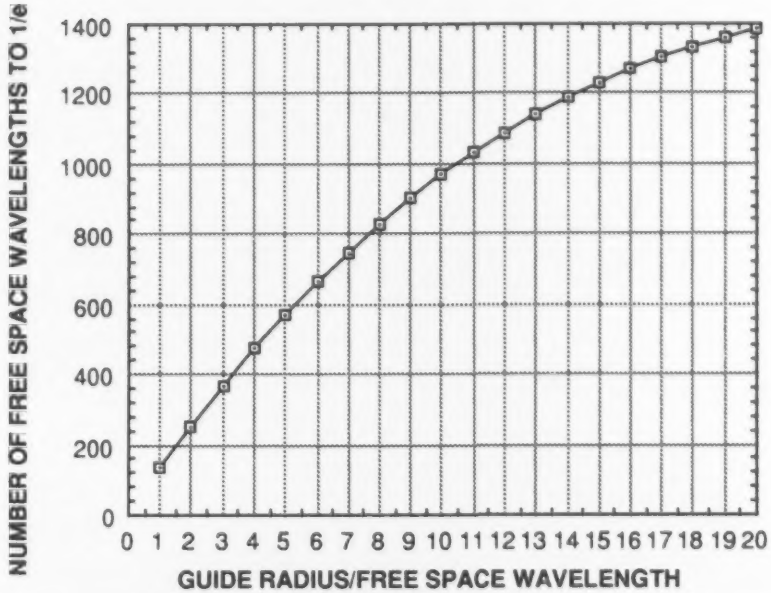

Fig.8 Propagation Distance of the TM_{01} Mode at 1.033 μm

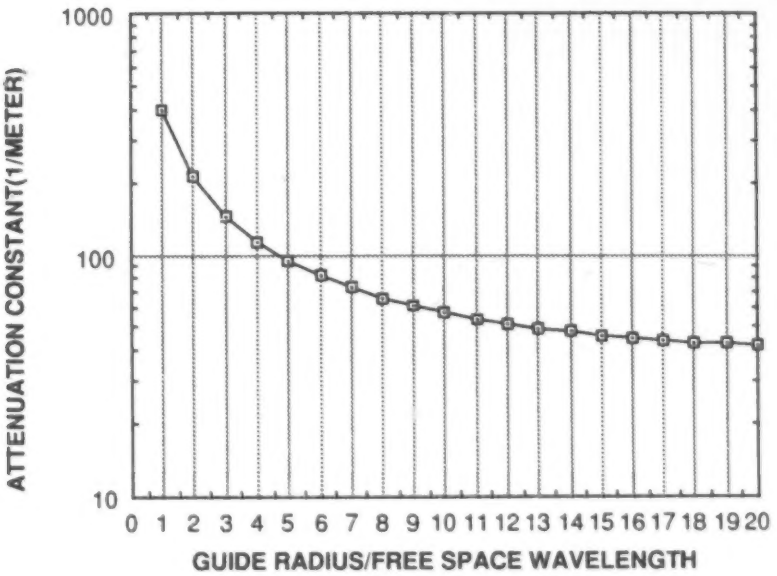

Fig.9 Attenuation Constant of the TM_{01} Mode at 9.919 μm

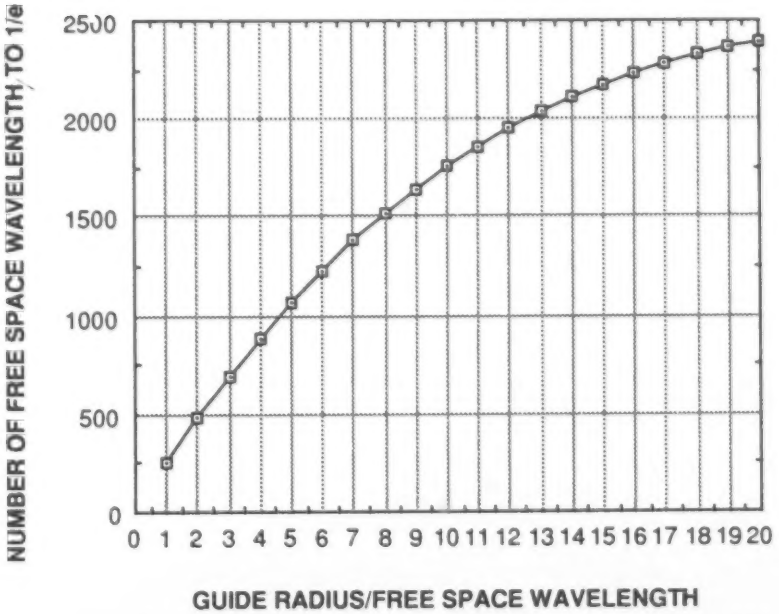
NUMBER OF FREE SPACE WAVELENGTH TO 1/e
2500
2000
1500
1000
500
0
0 1 2 3 4 5 6 7 8 9 10 11 12 13 14 15 16 17 18 19 20
GUIDE RADIUS/FREE SPACE WAVELENGTH

Fig.10 Propagation Distance of the TM_{01} Mode at 9.919 μm

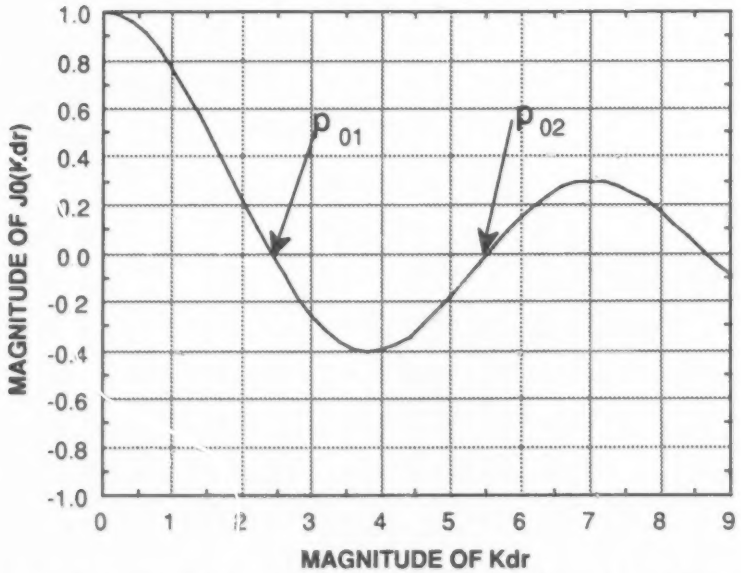

Fig.11 Radial Variation of E_{zd} of the Ideal Lossless Waveguide for the TM_{01} Mode

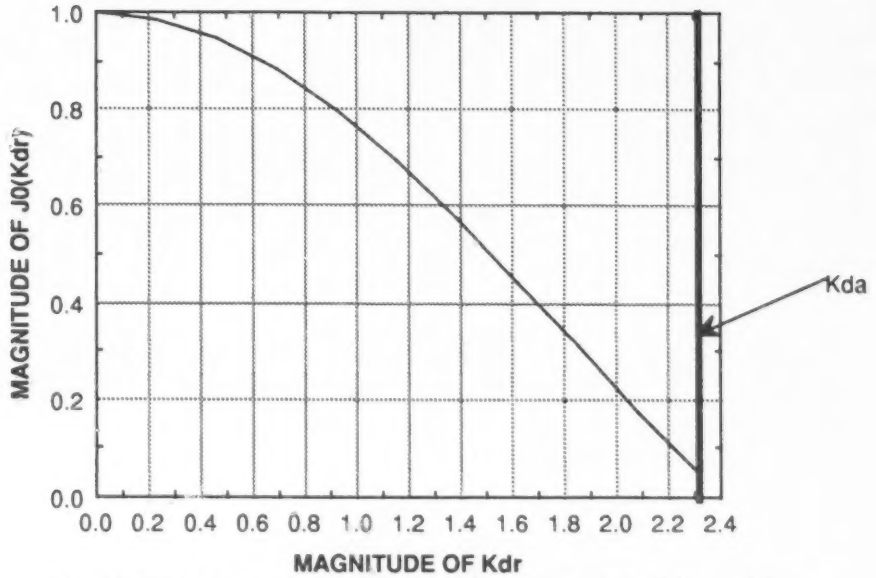

Fig.12 Radial Variation of E_{zd} of theMicrostructural Waveguide for the TM01 Mode at 1.033 μm and $a/\lambda_0=1$

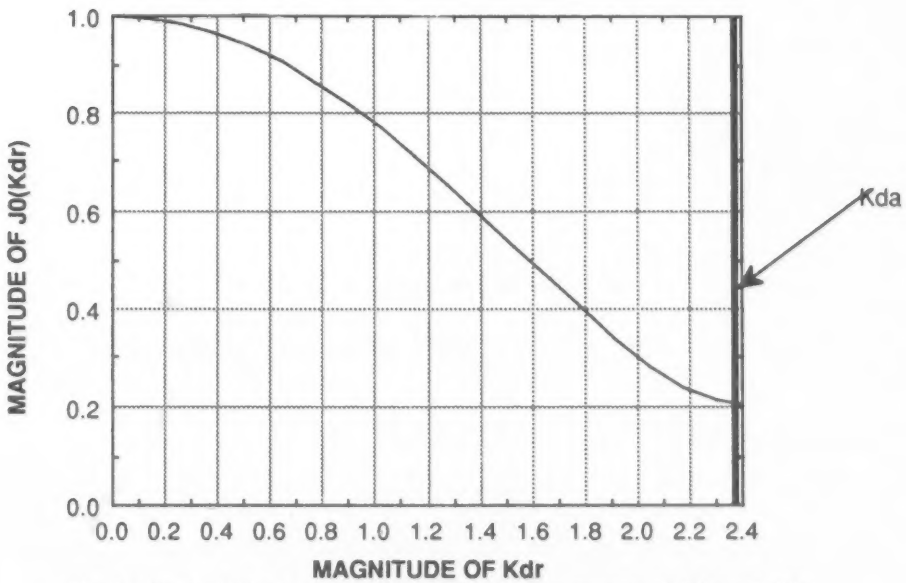

Fig.13 Radial Variation of E_{zd} of the Microstructural Waveguide for the TM01 Mode at 1.033 μm and $a/\lambda_0=20$

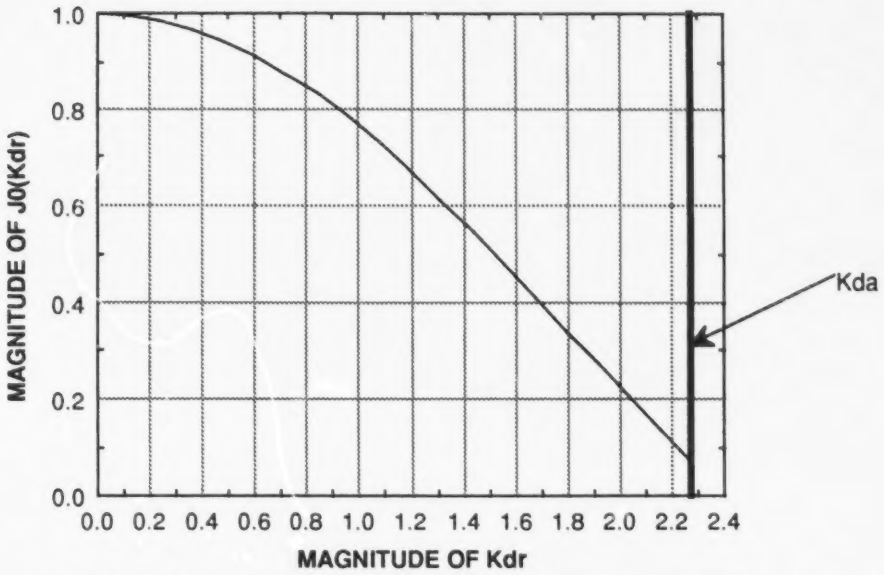

Fig.14 Radial Variation of E_{zd} of the Microstructural Waveguide for the TM01 Mode at 9.919 μm and $a/\lambda_0=1$

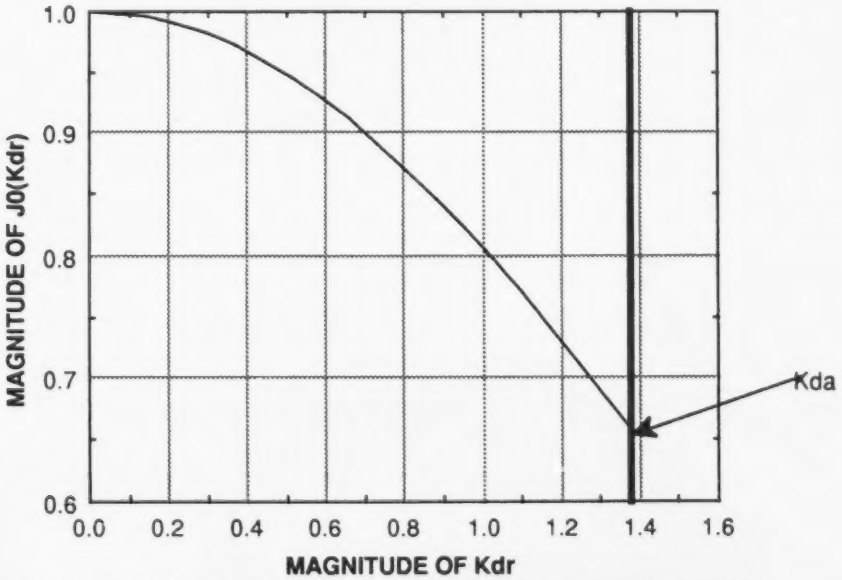

Fig.15 Radial Variation of E_{zd} of the Microstructural Waveguide for the TM01 Mode at 9.919 μm and $a/\lambda_0=20$

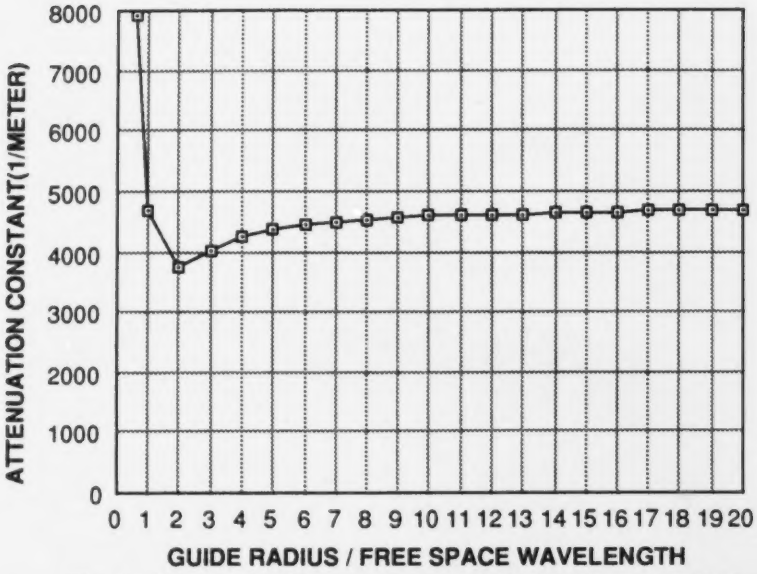

Fig.16 Attenuation Constants of the Hybrid Mode at 1.033μm

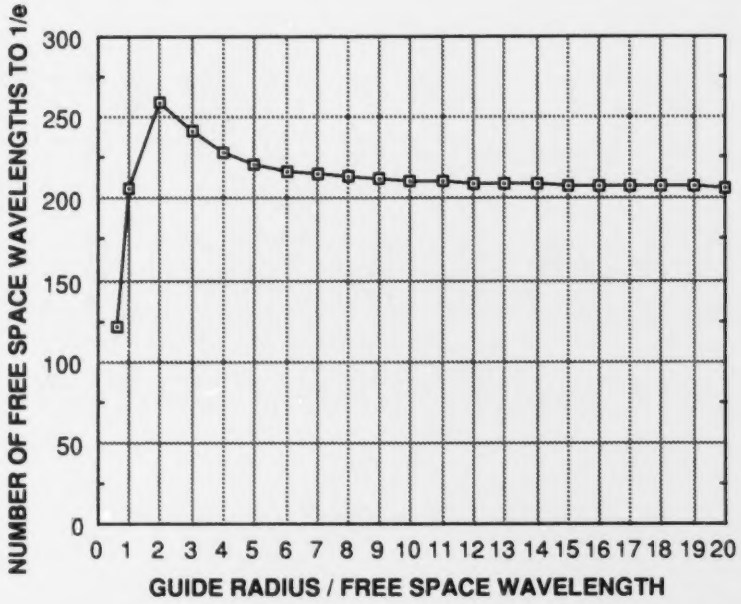
NUMBER OF FREE SPACE WAVELENGTHS TO 1/e
300
250
200
150
100
50
0
0 1 2 3 4 5 6 7 8 9 10 11 12 13 14 15 16 17 18 19 20
GUIDE RADIUS / FREE SPACE WAVELENGTH

Fig.17 Propagation Distance of the Hybrid Mode at 1.033μm

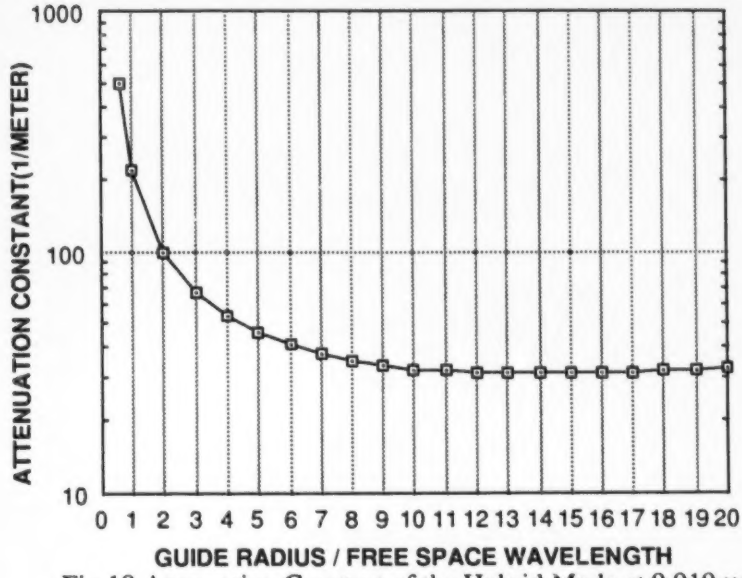

Fig.18 Attenuation Constant of the Hybrid Mode at 9.919 μm

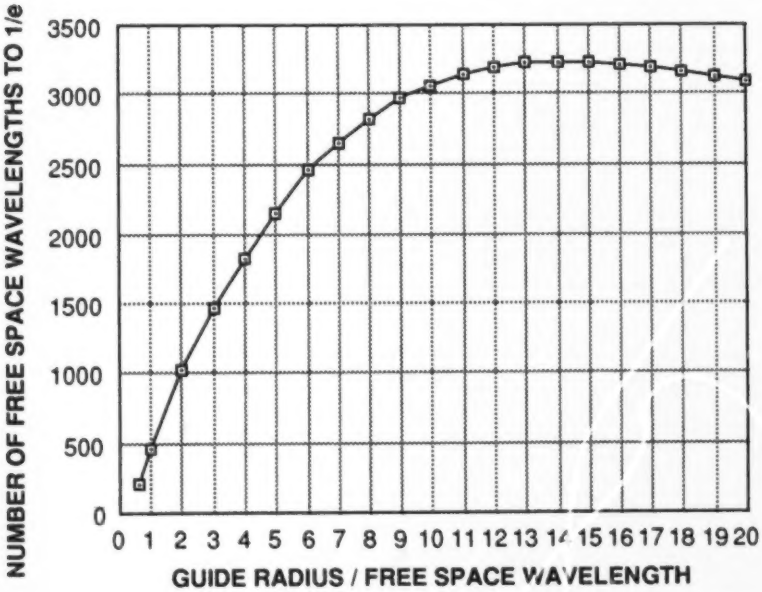

Fig.19 Propagation Distance of the Hybrid Mode at 9.919 μm

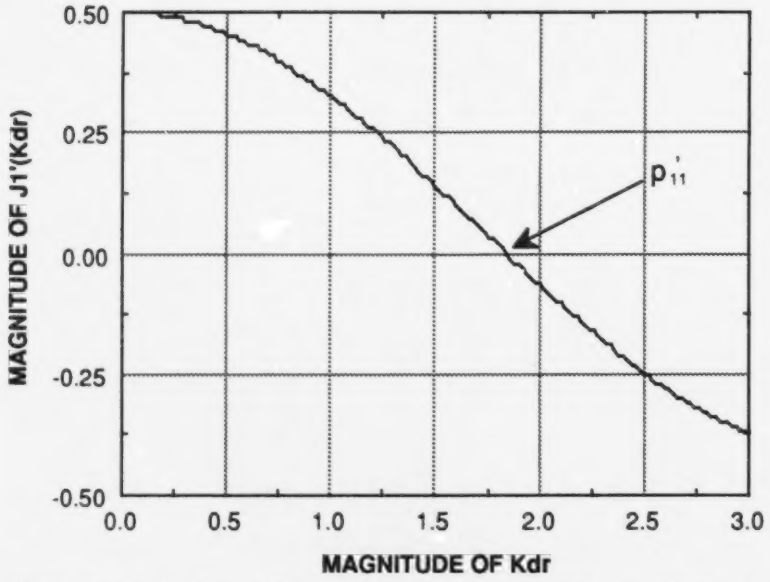

Fig.20 Radial Variation of $E_{\phi d}$ of the Ideal Lossless Waveguide for the TE_{11} Mode

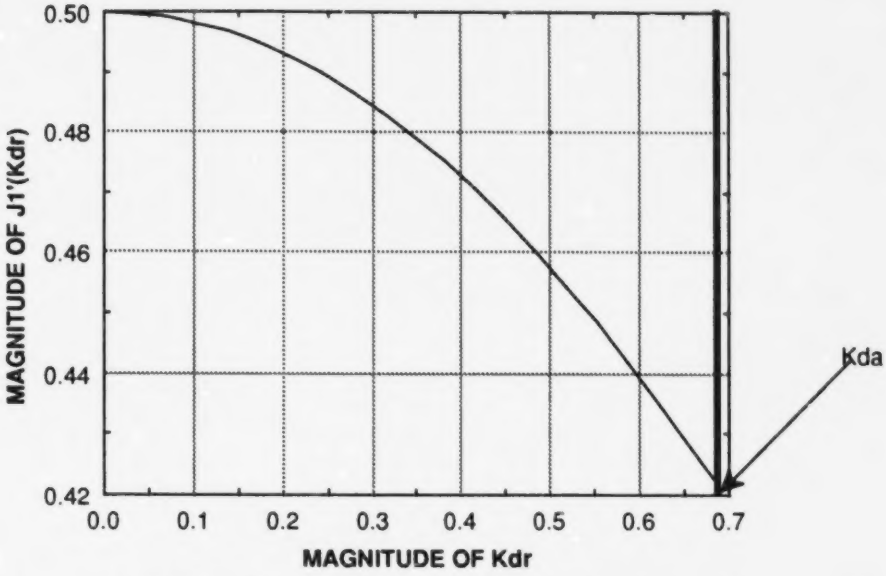

Fig. 21 The Magnitude of J_1' (Kdr) of the Microstructural Waveguide for the Hybrid Mode at 1.033μm and $a/\lambda_0=2$

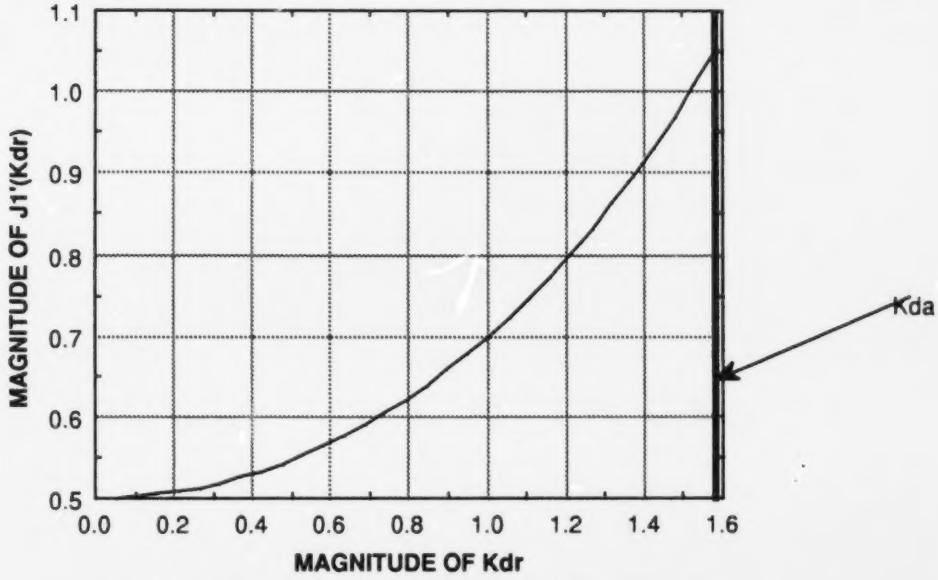

Fig. 22 The Magnitude of J_1' (Kdr) of the Microstructural Waveguide for the Hybrid Mode at 1.033μm and $a/\lambda_0=3$

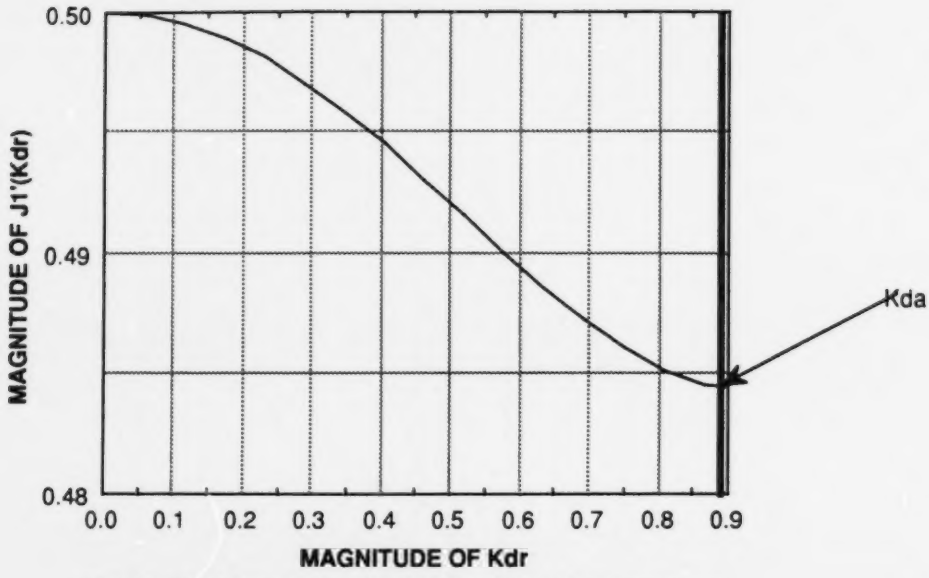

Fig.23 The Magnitude of J_1' (Kdr) of the Microstructural Waveguide for the Hybrid Mode at 9.919μm and $a/\lambda_0=18$

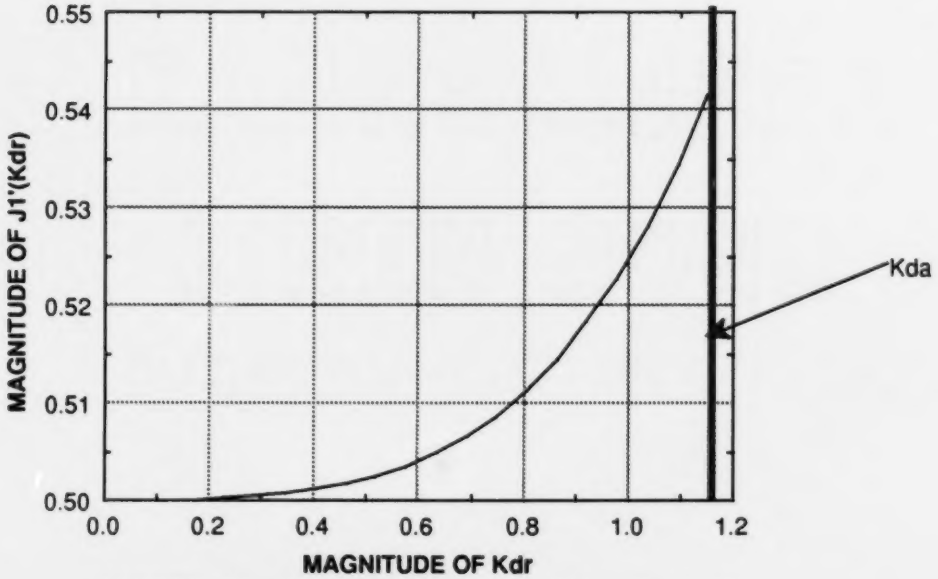

Fig.24 The Magnitude of J_1' (Kdr) of the Microstructural Waveguide for the Hybrid Mode at 9.919μm and $a/\lambda_0=19$

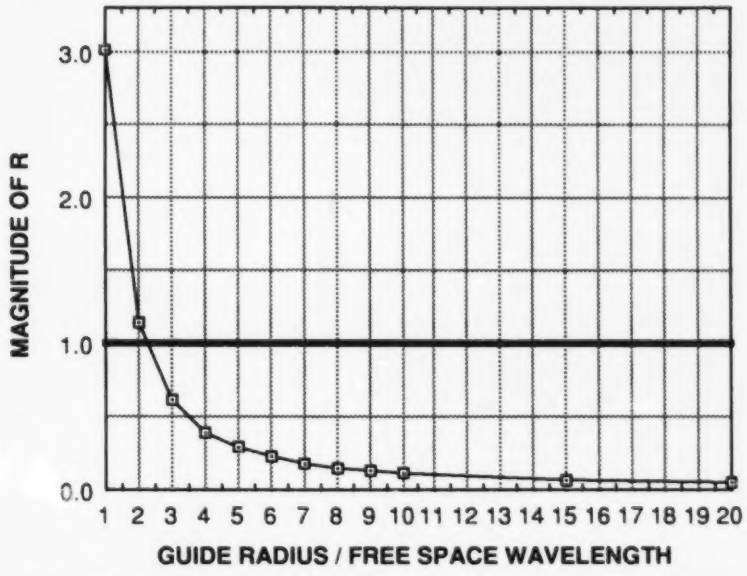

Fig.25 Magnitude of R for the Hybrid Mode at 1.033μm

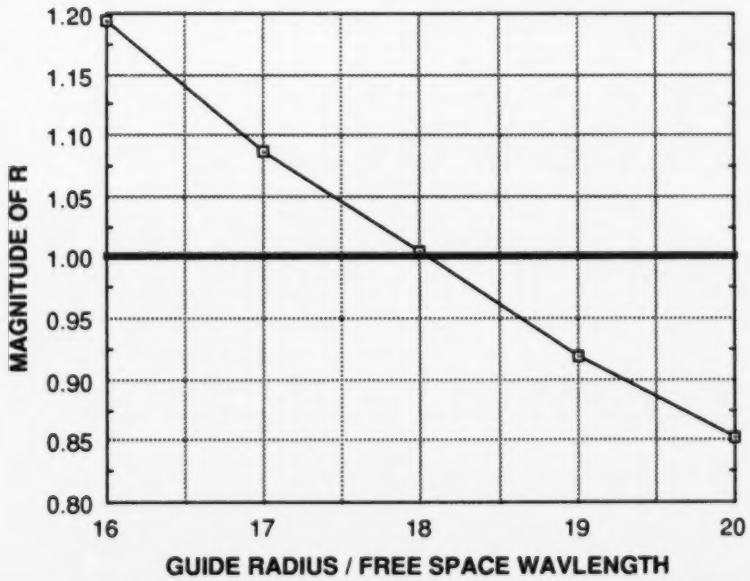

Fig.26 Magnitude of R for the Hybrid Mode at 9.919μm

REFERENCES

[1] K. E. Peterson, "Silicon as a mechanical material", *Proc. IEEE*, vol. 70, pp. 420-451, 1982.

[2] J. B. Angell, S. C. Terry, and P. W. Barth, "Silicon micromechanical devices", *Sci. Amer.*, vol. 248, pp. 44-55, Apr. 1983.

[3] M. Parameswaran, H. P. Baltes, Lj. Ristic, A. C. Dhaded, and A. M. Robinson, "A new approach for the fabrication of micromechanical structures", *Sensors and Actuators*, vol. 19, pp. 289-307, 1989.

[4] H. Baltes, E. Charbon, M. Parameswaran, and A. M. Robinson, "Humidity sensitive oscillator fabricated in double poly CMOS technology", *Sensors and Actuators*, vol. B1, pp. 441-445, 1990.

[5] R. T. Howe, "Resonant microstructures", *Tech. Dig. Papers, IEEE Int. Conf. on Solid State Sensors and Actuators, Transducers'87*, (Tokyo, Japan), pp. 843-848, 1987.

[6] R. G. Johnson and R. E. Higashi, "A microbridge air-flow sensor", *Scientific Honeyweller*, vol. 8, pp. 23-28, 1987.

[7] S. E. Miller, "Integrated optics: An introduction", *Bell Syst. Tech. J.*, vol. 48, pp. 2059-2069, 1969.

[8] J. E. Goell, "Rib waveguide for integrated circuits", *Appl. Opt.*, vol. 12, pp. 2797-2798, 1973.

[9] H. Furuta, H. Noda, and A. Ihaya, "Novel optical waveguide for integrated optics", *Appl. Opt.*, vol. 13, pp. 322-326, 1974.

[10] S. Somekh, E. Garmire, A. Yariv, H. L. Garvin, and R. G. Hunsperger, "Channel optical waveguides and directional couplers in GaAs-imbedded and ridged", *Appl. Opt.*, vol. 13, pp. 327-330, 1974.

[11] F. S. Hickernell, "Optical waveguides on silicon", *Solid State Technol.*, vol. 31, pp. 83-88, Nov. 1988.

[12] W. T. Tsang, C. C. Tseng, and S. Wang, "Optical waveguides fabricated by preferential etching", *Appl. Opt.*, vol. 14, pp. 1200-1260, 1975.

[13] C. C. Tseng, D. Botez, and S. Wang, "Optical bends and rings fabricated by preferential etching", *Appl. Phys. Lett.*, vol. 26, pp. 699-701, 1975.

[14] C. Hu and S. Kim, "Thin-film dye laser with etched cavity", *Appl. Phys. Lett.*, vol. 29, pp. 582-585, 1976.

[15] J. Brodie, "Physical considerations in vacuum microelectronics devices", *IEEE Trans. Electron. Dev.*, vol. 36, pp. 2641-2644, 1989.

[16] W. J. Orvis, C. F. McConaghy, D. R. Ciarlo, J. H. Yee, and E. W. Hee, "Modeling and fabricating micro-cavity integrated Vacuum tubes", *IEEE Trans. Electon. Dev.*, vol. 36, pp. 2651-2658, 1989.

[17] J. R. Carson, S. P. Mead, and S. A. Schelkunoff, "Hyper-frequency transmission", *Bell Syst. Tech. J.*, vol. 15,

pp. 310-327, 1936.

[18] E. A. J. Marcatilli and R. A. Schmeltzer, "Hollow metallic and dielectric waveguides for long distance optical transmission and lasers", *Bell Syst. Tech. J.*, vol. 43, pp. 1783-1809, Jul. 1964.

[19] H. Nishihara, T. Inoue, and J. Koyama, "Low-loss parallel-plate waveguides at 10.6 μm", *Appl. Phys. Lett.*, vol. 25, pp. 391-393, 1974.

[20] E. Garmire, T. McMahon, and J. Koyama, "Propagation of infrared light in flexible hollow waveguides", *Appl. Opt.*, vol. 15, pp. 145-150, 1976.

[21] E. Garmire, "Propagation of ir light in flexible hollow waveguides: further discussion", *Appl. Opt.*, vol. 15, pp. 3037-3039, 1976.

[22] F. E. Vermeulen, C. R. James, and A. M. Robinson, "Hollow microstructural waveguide for propagation of infrared radiation", *J. Lightwave Technol.*, vol. 9, pp. 1053-1060, 1991.

[23] S. Ramo, J. R. Whinnery, and T. Van Duzer, *Fields and Waves in Communication Electronics*. New York: Wiley, 1984.

[24] R. M. A. Azzam and N. M. Bashara, *Ellipsometry and Polarized Light*. Amsterdam: North-Holland, 1977.

[25] E. D. Palik, *Handbook of Optical Constants of Solids*. Orlando: Academic, 1985.

[26] A. B. Bronwell and R. E. Beam, *Theory and Application of Microwaves*. New York: McGraw-Hill, 1947.

[27] N. W. McLachlan, *Bessel Functions for Engineers.* Oxford: Clarendon Press, 1961.

[28] G. N. Watson, *A Treatise on the Theory of Bessel Functions.* Cambridge: cambridge University Press, 1966 .

APPENDIX

FURTHER ANALYSIS OF SOME SPECIAL CASES

In Chapter 4, the following inequality was used,

$$\sqrt{\varepsilon_m/\varepsilon_o} \gg a/\lambda_o$$

When this inequality holds, both the perturbation and power flow methods can be used to obtain the propagation characteristics.

For a microwave waveguide, since the refractive index is infinite for metal at microwave frequencies, $\sqrt{\varepsilon_m/\varepsilon_o} \gg a/\lambda_o$ naturally holds.

For a microstructural waveguide, this relationship does not hold for λ_o of interest in this thesis. But it can hold if we choose λ_o so that a/λ_o is much less than 1.

According to the analysis in Chapter 4, if $\sqrt{\varepsilon_m/\varepsilon_o} \gg a/\lambda_o$ holds there exist TM modes and TE modes only.

The purpose of analysis of such special case are: I. These results can be used as initial estimates for finding the propagation constant γ using Muller's method, which we discussed in detail in Chapter 5.

II. We can have a deeper understanding of special features of microstructural waveguides.

A.1 Analysis of TE Modes

We know that[23]:

$$J_m''(p_{mn}) = \frac{m^2 - p_{mn}^2}{p_{mn}^2} J_m(p_{mn}) \quad .....(A.1.1)$$

In the determinantal equation (4.3.2), making a Taylor series expansion of $J_m'(K_d a)$ around p_{mn}, and substituting $K_d = p_{mn}/a$ into all the terms other than $J_m'(K_d a)$, we have

$$J_m'(K_d a) \cong (K_d a - p_{mn}) J_m''(p_{mn})$$

Hence, from (A.1.1), the determinantal equation becomes

$$(K_d a - p_{mn}) \frac{m^2 - p_{mn}^2}{p_{mn}^2} = j\frac{p_{mn}}{ka} \frac{1}{n-jk} + j\frac{ka}{p_{mn}} m^2 \left(1 - \left(\frac{p_{mn}}{ka}\right)^2\right) \frac{1}{p_{mn}^2} \frac{1}{n-jk}$$

Therefore,

$$(K_d a - p_{mn}) = j\frac{p_{mn}^2}{m^2 - p_{mn}^2} (p_{mn}/ka) \frac{1}{n-jk} + j\frac{m^2}{m^2 - p_{mn}^2}\left((ka/p_{mn}) - (p_{mn}/ka)\right) \frac{1}{n-jk}$$

$$= -j(p_{mn}/ka) \frac{1}{n-jk} + j\frac{m^2}{m^2 - p_{mn}^2} (ka/p_{mn}) \frac{1}{n-jk}$$

i.e.

$$K_d = (p_{mn}/a) - j(p_{mn}/ka^2) \frac{1}{n-jk} + j\frac{m^2}{m^2 - p_{mn}^2} (k/p_{mn}) \frac{1}{n-jk}$$

Thus, we have:

$$K_d^2 = \left((p_{mn}/a) - j(p_{mn}/ka^2) \frac{1}{n-jk} + j\frac{m^2}{m^2 - p_{mn}^2} (k/p_{mn}) \frac{1}{n-jk} \right)^2$$

which can be written as,

$$K_d^2 = k^2\left[(p_{mn}/ak) - j(p_{mn}/k^2a^2)\frac{1}{n-jk} + j\frac{m^2}{m^2 - p_{mn}^2}(1/p_{mn})\frac{1}{n-jk}\right]^2$$

Keeping in mind that $k = \frac{2\pi}{\lambda_o}$, the above can be substituted into the following,

$$\gamma^2 = -k^2 + K_d^2,$$

Hence it is straightforward to obtain

$$\gamma^2 = -k^2 + k^2\left[(\frac{p_{mn}\lambda_o}{2\pi a}) - j(\frac{p_{mn}\lambda_o}{2\pi a})^2(1/p_{mn})\frac{1}{n-jk} + j\frac{m^2}{m^2 - p_{mn}^2}(1/p_{mn})\frac{1}{n-jk}\right]^2$$

$$= -k^2\left[1 - (\frac{p_{mn}\lambda_o}{2\pi a})^2\left(1 - j(\frac{p_{mn}\lambda_o}{2\pi a})(1/p_{mn})\frac{1}{n-jk} + j\frac{m^2}{m^2 - p_{mn}^2}(2\pi a/p_{mn}^2\lambda_o)\frac{1}{n-jk}\right)^2\right]$$

We only consider one term of the right-hand side of the above. We can show that

$$\left(1 - j(\frac{p_{mn}\lambda_o}{2\pi a})(1/p_{mn})\frac{1}{n-jk} + j\frac{m^2}{m^2 - p_{mn}^2}(2\pi a/p_{mn}^2\lambda_o)\frac{1}{n-jk}\right)^2$$

$$= \left(1 - j(\frac{p_{mn}\lambda_o}{2\pi a})(1/p_{mn})\frac{1}{n-jk}\right)^2$$

$$+ 2\left(1 - j(\frac{p_{mn}\lambda_o}{2\pi a})(1/p_{mn})\frac{1}{n-jk}\right)\left(j\frac{m^2}{m^2 - p_{mn}^2}(2\pi a/p_{mn}^2\lambda_o)\frac{1}{n-jk}\right)$$

$$+ \left(j\frac{m^2}{m^2 - p_{mn}^2}\right)^2(2\pi a/p_{mn}^2\lambda_o)^2\left(\frac{1}{n-jk}\right)^2$$

Further, the right-hand side of the above can be

written as,

$$1-2j\left(\frac{p'_{mn}\lambda_o}{2\pi a}\right)(1/p'_{mn})\frac{1}{n-jk} + j^2\left(\frac{p'_{mn}\lambda_o}{2\pi a}\right)^2(1/p'_{mn})^2\left(\frac{1}{n-jk}\right)^2$$

$$+2\left(j\frac{m^2}{m^2-p'^2_{mn}}(2\pi a/p'^2_{mn}\lambda_o)\frac{1}{n-jk}\right) - 2j^2\frac{m^2}{m^2-p'^2_{mn}}(1/p'^2_{mn})\left(\frac{1}{n-jk}\right)^2$$

$$+\left(j\frac{m^2}{m^2-p'^2_{mn}}\right)^2(2\pi a/p'^2_{mn}\lambda_o)^2\left(\frac{1}{n-jk}\right)^2$$

Since $\left(\frac{1}{n-jk}\right)^2$ is very small and we know $n-jk \gg a/\lambda_o$, neglecting terms of the order of $\left(\frac{1}{n-jk}\right)^2$, the above can be further simplified to

$$1-2j\left(\frac{p'_{mn}\lambda_o}{2\pi a}\right)(1/p'_{mn})\frac{1}{n-jk} + 2\left(j\frac{m^2}{m^2-p'^2_{mn}}(2\pi a/p'^2_{mn}\lambda_o)\frac{1}{n-jk}\right)$$

Hence, we obtain,

$$\gamma^2 \cong -k^2\left[1-\left(\frac{p'_{mn}\lambda_o}{2\pi a}\right)^2+2j\left(\frac{p'_{mn}\lambda_o}{2\pi a}\right)^2(1/ak)\frac{1}{n-jk} + 2j\frac{m^2}{p'^2_{mn}-m^2}(1/ak)\frac{1}{n-jk}\right]^2$$

Thus,

$$\gamma = -jk\left[1-\left(\frac{p'_{mn}\lambda_o}{2\pi a}\right)^2+2j\left(\frac{p'_{mn}\lambda_o}{2\pi a}\right)^2(1/ak)\frac{1}{n-jk} + 2j\frac{m^2}{p'^2_{mn}-m^2}(1/ak)\frac{1}{n-jk}\right]^{1/2} \quad \ldots.(A.1.2)$$

For reasonably small m, and since $n-jk \gg a/\lambda_o$

$$\left|1-\left(\frac{p'_{mn}\lambda_o}{2\pi a}\right)^2\right| \gg \left|2j\left(\frac{p'_{mn}\lambda_o}{2\pi a}\right)^2(1/ak)\frac{1}{n-jk} + 2j\frac{m^2}{p'^2_{mn}-m^2}(1/ak)\frac{1}{n-jk}\right|$$

Then, since $\alpha = \mathrm{Re}(\gamma)$, we obtain,

$$\alpha = \frac{1}{a}\frac{n}{n^2+k^2}\left(\left(\frac{p'_{mn}\lambda_o}{2\pi a}\right)^2 + \frac{m^2}{p'^2_{mn}-m^2}\right)\Big/\left(1-\left(\frac{p'_{mn}\lambda_o}{2\pi a}\right)^2\right)^{1/2}$$

A.2 Analysis of TM Modes

In the determinantal equation (4.3.3), we make a Taylor series expansion around the root of $J_m(x)=0$, p_{mn}. Substituting $K_d = p_{mn}/a$ into all terms in the equation except $J_m(K_d a)$, we obtain,

$$J_m(K_d a) = J_m(p_{mn}) + (K_d a - p_{mn})J_m'(K_d a) ,$$

Therefore, the determinantal equation becomes

$$\frac{1}{K_d a - p_{mn}} = j\frac{p_{mn}}{ka}(n-jk)$$

Then, we have

$$K_d = \frac{p_{mn}}{a} + \frac{k}{jp_{mn}}\frac{1}{n-jk}$$

Thus,

$$K_d^2 = k^2\left(\frac{p_{mn}}{ak} + \frac{1}{jp_{mn}}\frac{1}{n-jk}\right)^2$$

Since $k=2\pi/\lambda_o$,

$$\gamma^2 = -k^2 + K_d^2 = -k^2\left[1 - \left(\frac{p_{mn}\lambda_o}{2\pi a}\right)^2\left(1+\frac{2\pi a}{jp^2_{mn}\lambda_o}\frac{1}{n-jk}\right)^2\right]$$

$$= -k^2\left[\left(1 - \left(\frac{p_{mn}\lambda_o}{2\pi a}\right)^2\right) - \frac{\lambda_o}{j\pi a}\frac{1}{n-jk} - (1/jp^2_{mn})\left(\frac{1}{n-jk}\right)^2\right]$$

Because the term with the factor $(\frac{1}{n-jk})^2$ is much smaller than the other terms present we obtain

$$\gamma^2 \cong -k^2\left[(1 - (\frac{p_{mn}\lambda_o}{2\pi a})^2) - \frac{\lambda_o}{j\pi a}\frac{1}{n-jk}\right]$$

Thus, we can get

$$\gamma \cong jk\left[(1 - (\frac{p_{mn}\lambda_o}{2\pi a})^2) - \frac{\lambda_o}{j\pi a}\frac{1}{n-jk}\right]^{1/2}$$

For reasonably small p_{mn}

$$|(1 - (\frac{p_{mn}\lambda_o}{2\pi a})^2)| \gg |\frac{\lambda_o}{j\pi a}\frac{1}{n-jk}|$$

Thus,

$$\gamma = jk\left[(1 - (\frac{p_{mn}\lambda_o}{2\pi a})^2)^{1/2} - \frac{1}{2}(1 - (\frac{p_{mn}\lambda_o}{2\pi a})^2)^{-1/2}\frac{\lambda_o}{j\pi a}\frac{1}{n-jk}\right] \quad .....(A.2.1)$$

again since $\alpha = Re(\gamma)$

$$\alpha = \frac{1}{a}\frac{n}{n^2+k^2}\left(1/\sqrt{1-(\frac{p_{mn}\lambda_o}{2\pi a})^2}\right)$$

A.3 Comments On The Results

The methods used here are of interest in the analysis of waveguides, even though this derivation is not the main purpose of this thesis.

In summary the relation between refractive index $\sqrt{\varepsilon_m/\varepsilon_o}$ and a/λ_o is,

for a radio or microwave waveguide,

$$\sqrt{\varepsilon_m/\varepsilon_o} \gg a/\lambda_o$$

for an optical waveguides of large dimensions,

$$\sqrt{\varepsilon_m/\varepsilon_o} \ll a/\lambda_o$$

for a microstructural waveguide,

$$\sqrt{\varepsilon_m/\varepsilon_o} \Leftrightarrow a/\lambda_o$$

This latter relationship means that terms are of the same order of magnitude

It is readily seen that we have studied the case of wave propagation which is mathematically the most difficult. The microwave case and the large optical case are special limits of the case investigated in this thesis.